
Volume 249 Issue 6 September 15, 2010 ISSN 0022-0396
ELSEVIER
JOURNAL OF
DIFFERENTIAL
EQUATIONS
Editors-in-Chief
Shui-Nee Chow
John Mallet-Paret
Konstantin Mischaikow
Founding Editors
Jack K. Hale
J. P. LaSalle
Editorial Board
Sigurd Angenent
John Ball
Alberto Bressan
Courtney Coleman
Avner Friedman
Kening Lu
W.-M. Ni
Czesław Olech
James Serrin
Marshall Slemrod
Walter Strauss
Roger Temam
Sijue Wu
Yingfei Yi

J. Differential Equations 249 (2010) 1410–1435

Contents lists available at ScienceDirect

Journal of Differential Equations

www.elsevier.com/locate/jde

Versal unfoldings of predator–prey systems with ratio-dependent functional response ☆

Shigui Ruan [a,*], Yilei Tang [b], Weinian Zhang [c]

[a] Department of Mathematics, University of Miami, Coral Gables, FL 33124-4250, USA
[b] Department of Mathematics, Shanghai Jiao Tong University, Minhang, Shanghai 200240, PR China
[c] Department of Mathematics, Sichuan University, Chengdu, Sichuan 610064, PR China

ARTICLE INFO

Article history:
Received 17 October 2008
Revised 8 January 2010

MSC:
34C05
34C60
92D25

Keywords:
Predator–prey system
Versal unfolding
Normal form
Degenerate equilibrium
Heteroclinic loop
Bifurcation

ABSTRACT

In this paper we study the versal unfolding of a predator–prey system with ratio-dependent functional response near a degenerate equilibrium in order to obtain all possible phase portraits for its perturbations. We first construct the unfolding and prove its versality and degeneracy of codimension 2. Then we discuss all its possible bifurcations, including transcritical bifurcation, Hopf bifurcation, and heteroclinic bifurcation, give conditions of parameters for the appearance of closed orbits and heteroclinic loops, and describe the bifurcation curves. Phase portraits for all possible cases are presented.

1. Introduction

The dynamics of predator–prey systems has been favored by both biologists and mathematicians since the well-known Lotka–Volterra model was brought forward (see [9,21]). Functional response is a crucial and important concept in modeling predator–prey interactions, which describes the change in the density of prey per unit time per predator. Traditionally, the functional response is regarded as

☆ Research was partially supported by NSF grant DMS-0715772 (S.R.), NSFC grant 10801095 (Y.T.), and NSFC grant 0825104 and SRFDP grant 200806100002 (W.Z.).

* Corresponding author.
E-mail address: ruan@math.miami.edu (S. Ruan).

0022-0396/$ – see front matter
doi:10.1016/j.jde.2010.06.015

a function of the prey density and is called a *prey-dependent functional response*. A typical example is the Michaelis–Menten or Holling type II function $p(x) = cx/(x+m)$ (see [9,21]).

It has been noticed that predator–prey models with prey-dependent functional response cannot explain the experimental observations that the predators or both the predators and prey can either go extinction or coexist in oscillatory modes depending on the initial populations densities (see [14,20]). Also, such models cannot produce the so-called "paradox of biological control" phenomenon: durable coexistence of prey with their predators at a mean abundance is much lower than the prey carrying capacity (see [19,1]). To address these issues, Arditi and Ginzburg [2] suggested that the functional response should be expressed in terms of the ratio of prey to their predators which is now called the *ratio-dependent functional response*. Based on the Michaelis–Menten or Holling type II function, they proposed the following ratio-dependent predator–prey model

$$\begin{cases} \dfrac{dx}{dt} = x\left(a - bx - \dfrac{cy}{x+my}\right), \\ \dfrac{dy}{dt} = y\left(-d + \dfrac{fx}{x+my}\right), \end{cases} \tag{1.1}$$

where $x(t)$ and $y(t)$ are the density of prey and predators at time t, respectively. All parameters are positive constants, a is the prey intrinsic growth rate, a/b is the carrying capacity of the prey, c represents the capturing rate of predators, d denotes the death rate of predators, f is the conversion rate, and m is the half saturation constant. In the last decade, many researchers (e.g. [4,5,13,17,18,22, 26]) have paid their attention to this model and many interesting and novel dynamic behaviors have been observed.

With the change of variables $x \mapsto (a/b)x$, $y \mapsto (a/mb)y$, $t \mapsto (m/c)t$ and the transformation of parameters $\alpha = ma/c$, $\beta = md/c$, $\kappa = mf/c$, system (1.1) can be transformed into an equivalent form

$$\begin{cases} \dfrac{dx}{dt} = \alpha x(1-x) - \dfrac{xy}{x+y}, \\ \dfrac{dy}{dt} = -\beta y + \dfrac{\kappa xy}{x+y}, \end{cases} \tag{1.2}$$

which in turn is orbitally equivalent to the following system

$$\begin{cases} \dfrac{dx}{dt} = x\{\alpha x + (\alpha - 1)y - \alpha x^2 - \alpha xy\}, \\ \dfrac{dy}{dt} = y\{(\kappa - \beta)x - \beta y\} \end{cases} \tag{1.3}$$

after the re-scaling of the time variable $d\tau = (x+y)\,dt$, where $x, y \geqslant 0$ and α, β, κ are all positive. Notice that system (1.3) is of Lotka–Volterra type.

System (1.3) has three equilibria $(0,0)$, $(1,0)$ and (x^*, y^*) in the first quadrant, where $x^* = (\alpha\kappa - \kappa + \beta)/\alpha\kappa$, $y^* = (\kappa - \beta)\bar{x}/\beta$. The origin $(0,0)$ is degenerate and great efforts [4,13,15,17,26] have been made to understand its qualitative properties by means of Briot–Bouquet transformations and generalized normal sectors. Transcritical bifurcation at $(1,0)$ and Hopf bifurcation at (x^*, y^*) have also been discussed. The existence of a heteroclinic orbit connecting the equilibria $(1,0)$ and $(0,0)$ was proposed in [13] and discussed in [4,26]. Heteroclinic orbits have been further studied by combining analytical method and numerical approach in [4,18,22,25].

The above mentioned bifurcations are induced by the change of parameters within system (1.2). Actually, having so much degeneracy the system may be affected by other changes from outside but within Lotka–Volterra systems. This motivates us to unfold bifurcations of the system completely near the degenerate origin and display all possible phase portraits arising from perturbations in the class of generalized Lotka–Volterra systems (called *GLV systems* for abbreviation)

$$\begin{cases} \dfrac{dx}{dt} = xP(x, y), \\ \dfrac{dy}{dt} = yQ(x, y), \end{cases} \tag{1.4}$$

where both $P(x, y)$ and $Q(x, y)$ are analytic functions.

In this paper we study the versal unfolding of system (1.3) near $(0,0)$ in the class of GLV systems. We first reduce system (1.3) to a normal form and prove that its degeneracy is of codimension 2. Then we present a versal unfolding for the system, study qualitative properties of the unfolding in various cases, and discuss all possible bifurcations including transcritical bifurcation, Hopf bifurcation, bifurcations of periodic orbits and heteroclinic loops. We give conditions on system parameters for the appearance of closed orbits and heteroclinic loops and describe their bifurcation curves.

The rest of the paper is organized as follows. In Section 2 the system is reduced to its normal form. The versal unfolding is presented in Section 3. The existence and properties of equilibria of the versal unfolding are discussed in Section 4. Section 5 is devoted to the study of limit cycles, including the existence and uniqueness. Section 6 deals with the existence of heteroclinic loops. Bifurcation diagrams for all possible cases are given in Section 7.

2. Normal forms

The Jacobian matrix of system (1.3) at the origin $(0,0)$ is a zero matrix. We consider vector fields in the family of GLV systems (1.4) with the same degeneracy

$$\begin{cases} \dfrac{dx}{dt} = x\{a_{10}x + a_{01}y + a_{20}x^2 + a_{11}xy + a_{02}y^2 + O(|(x, y)|^3)\}, \\ \dfrac{dy}{dt} = y\{b_{10}x + b_{01}y + b_{20}x^2 + b_{11}xy + b_{02}y^2 + O(|(x, y)|^3)\}. \end{cases} \tag{2.1}$$

First, we reduce (2.1) to the simplest GLV system which is orbitally equivalent to (2.1).

Lemma 1. *Under the generic condition $a_{01}b_{01}(b_{01}b_{10} - 2b_{10}a_{01} + b_{01}a_{10}) \neq 0$, system (2.1) is orbitally equivalent to*

$$\begin{cases} \dfrac{dx}{dt} = x\{a_{10}x + a_{01}y + \tilde{a}_{20}x^2 + O(|(x, y)|^3)\}, \\ \dfrac{dy}{dt} = y\{b_{10}x + b_{01}y + O(|(x, y)|^3)\} \end{cases} \tag{2.2}$$

near the origin $(0,0)$.

Proof. We need to use transformations which do not change the structure of GLV systems. Such transformations can be chosen in the form

$$x = \tilde{x}(1 + c_1\tilde{x} + c_2\tilde{y}), \qquad y = \tilde{y}(1 + c_3\tilde{x} + c_4\tilde{y}), \qquad dt = (1 + c_5\tilde{x} + c_6\tilde{y})\,d\tilde{t}, \tag{2.3}$$

where the spatial part of the transformation $(x, y) \mapsto (\tilde{x}, \tilde{y})$ is close to the identity near the origin. Even if a constant c_0 is considered as one of its coefficients of degree 1, a simple dilation can reduce c_0 to 1. This transformation is obviously one-to-one near the origin, does not change the sign of time, and transforms system (2.1) into the following

$$\begin{cases} \dfrac{d\tilde{x}}{d\tilde{t}} = \tilde{x}\{a_{10}\tilde{x} + a_{01}\tilde{y} + \tilde{a}_{20}\tilde{x}^2 + \tilde{a}_{11}\tilde{x}\tilde{y} + \tilde{a}_{02}\tilde{y}^2 + O(|(\tilde{x},\tilde{y})|^3)\}, \\ \dfrac{d\tilde{y}}{d\tilde{t}} = \tilde{y}\{b_{10}\tilde{x} + b_{01}\tilde{y} + \tilde{b}_{20}\tilde{x}^2 + \tilde{b}_{11}\tilde{x}\tilde{y} + \tilde{b}_{02}\tilde{y}^2 + O(|(\tilde{x},\tilde{y})|^3)\}, \end{cases} \tag{2.4}$$

where

$$\begin{aligned} \tilde{a}_{20} &= a_{10}c_5 + a_{20}, \\ \tilde{a}_{02} &= -b_{01}c_2 + a_{01}c_4 + a_{01}c_6 + a_{02}, \\ \tilde{a}_{11} &= -a_{01}c_1 + (a_{10} - b_{10})c_2 + a_{01}c_3 + a_{01}c_5 + a_{10}c_6 + a_{11}, \\ \tilde{b}_{20} &= b_{10}c_1 - a_{10}c_3 + b_{10}c_5 + b_{20}, \\ \tilde{b}_{02} &= b_{01}c_6 + b_{02}, \\ \tilde{b}_{11} &= b_{10}c_2 + (b_{01} - a_{01})c_3 - b_{10}c_4 + b_{01}c_5 + b_{10}c_6 + b_{11}. \end{aligned}$$

In order to make (2.4) coincide with (2.2), it is required that

$$\tilde{a}_{11} = \tilde{a}_{02} = \tilde{b}_{20} = \tilde{b}_{11} = \tilde{b}_{02} = 0, \tag{2.5}$$

which is a system of linear equations in $(c_1, \dots, c_6)$. Under the condition that

$$W := a_{01}b_{01}(b_{01}b_{10} - 2b_{10}a_{01} + b_{01}a_{10}) \neq 0,$$

the coefficient matrix of system (2.5) has the same rank as its augmented matrix. Thus we can solve from system (2.5) that

$$\begin{aligned} c_1 = \{&2b_{10}^2a_{01}b_{02} + b_{01}^2a_{11}b_{10} - b_{01}a_{10}^2b_{02} - a_{01}b_{10}b_{11}b_{01} + 3a_{10}b_{10}a_{01}b_{02} - b_{10}^2a_{02}b_{01} \\ &- b_{01}b_{10}a_{10}b_{02} - a_{10}b_{10}a_{02}b_{01} + b_{01}a_{01}^2b_{20} - a_{01}b_{01}a_{11}b_{10} + a_{10}b_{01}^2a_{11} \\ &- a_{10}a_{01}b_{11}b_{01} + (b_{01}^2a_{10}^2 + b_{10}b_{01}^2a_{10} - 2a_{10}a_{01}b_{01}b_{10})c_2\}/W, \\ c_3 = \{&4b_{10}^2a_{01}b_{02} + b_{01}^2a_{11}b_{10} + b_{01}^2a_{01}b_{20} - 2a_{01}b_{10}b_{11}b_{01} - b_{01}b_{10}a_{10}b_{02} \\ &- 2b_{10}^2a_{02}b_{01} + (b_{10}b_{01}^2a_{10} + b_{10}^2b_{01}^2 - 2a_{01}b_{01}b_{10}^2)c_2\}/W, \\ c_4 = \{&a_{01}b_{02} - a_{02}b_{01} + b_{01}^2c_2\}/\{a_{01}b_{01}\}, \\ c_5 = \{&b_{10}^2a_{02}b_{01} - b_{01}^2a_{01}b_{20} - 2b_{10}^2a_{01}b_{02} - b_{01}^2a_{11}b_{10} + b_{01}b_{10}a_{10}b_{02} + a_{10}b_{10}a_{01}b_{02} \\ &+ a_{01}b_{10}b_{11}b_{01} - a_{10}b_{10}a_{02}b_{01} + b_{01}a_{01}^2b_{20} + a_{01}b_{01}a_{11}b_{10} - a_{10}a_{01}b_{11}b_{01}\}/W, \\ c_6 = -&b_{02}/b_{01}, \end{aligned}$$

where $c_2 \in \mathbf{R}$ can be chosen arbitrarily. Hence, an appropriate transformation (2.3) is determined, which transforms (2.1) into the normal form (2.2). □

Since system (2.1) has a zero matrix in its linear part, we cannot proceed the standard computation of normal forms (as shown in [6,10]) to simplify the system. From (2.4) we see that the transformation (2.3) does not change the coefficients $a_{10}, a_{01}, b_{10}, b_{01}$ of the terms of degree 2. We will concentrate on the generic case that none of $a_{10}, a_{01}, b_{10}, b_{01}$ is zero. In the opposite cases higher codimensions will be involved. In comparison with (2.1), system (2.2) clearly has the least number of coefficients and thus is called a *normal form* of (2.1), as being in the simplest form in the family of GLV systems reduced with the structure-preserving transformation (2.3) near the origin.

From Lemma 1, there remains a case that the generic condition is invalid, i.e.,

$$U_{20}(a_{10}, a_{01}, b_{10}, b_{01}) := b_{01}b_{10} - 2b_{10}a_{01} + b_{01}a_{10} = 0. \tag{2.6}$$

In this case our strategy is to give up the constant $\tilde{a}_{20}$ but retain one of others. If we retain $\tilde{a}_{11}$, similarly to (2.5) we obtain another linear system of $(c_1, \ldots, c_6)$ and the condition

$$U_{11}(a_{10}, a_{01}, b_{10}, b_{01}) := a_{01} - b_{01} \neq 0. \tag{2.7}$$

Retaining $\tilde{a}_{02}, \tilde{b}_{20}, \tilde{b}_{11}$, and $\tilde{b}_{02}$, we obtain the conditions

$$U_{02}(a_{10}, a_{01}, b_{10}, b_{01}) := a_{10} - b_{10} \neq 0, \tag{2.8}$$

$$V_{20}(a_{10}, a_{01}, b_{10}, b_{01}) = U_{11}(a_{10}, a_{01}, b_{10}, b_{01}) \neq 0, \tag{2.9}$$

$$V_{11}(a_{10}, a_{01}, b_{10}, b_{01}) = U_{02}(a_{10}, a_{01}, b_{10}, b_{01}) \neq 0, \tag{2.10}$$

$$V_{02}(a_{10}, a_{01}, b_{10}, b_{01}) := b_{01}a_{10} + a_{01}a_{10} - 2a_{01}b_{10} \neq 0, \tag{2.11}$$

respectively. It is easy to see that the polynomials U_{ij} and V_{ij} have common zeros in the subset

$$\mathcal{Z} := \left\{(a_{10}, a_{01}, b_{10}, b_{01}) \in \mathbf{R}_0^4\colon\ a_{01} = b_{01},\ a_{10} = b_{10}\right\}, \tag{2.12}$$

where $\mathbf{R}_0 := \mathbf{R}\backslash\{0\}$. Therefore, out of $\mathcal{Z}$ we can transform Eq. (2.1) into the simplest GLV system as in Lemma 1, where only one coefficient of degree 3 is retained. Concrete calculations show that the normal forms under (2.11) are same as the one given in Lemma 1 by the homeomorphism $(x, y) \mapsto (y, x)$. Similarly, the normal forms under (2.7) and (2.10) are the same and the normal forms under (2.8) and (2.9) are the same by $(x, y) \mapsto (y, x)$.

Applying Lemma 1 to our system (1.3), we obtain its normal form

$$\begin{cases} \dfrac{dx}{dt} = x\left\{\alpha x + (\alpha - 1)y + \tilde{a}_{20}x^2 + O\left(\left|(x, y)\right|^3\right)\right\}, \\ \dfrac{dy}{dt} = y\left\{(\kappa - \beta)x - \beta y + O\left(\left|(x, y)\right|^3\right)\right\}, \end{cases} \tag{2.13}$$

where

$$\tilde{a}_{20} = \frac{\alpha(\alpha^2\kappa + 2\alpha\beta - 3\alpha\kappa - 2\beta + \beta^2 - \beta\kappa + 2\kappa)}{(1 - \alpha)\{2(\alpha\kappa - \kappa + \beta) + \beta(\kappa - \alpha - \beta)\}} \tag{2.14}$$

under the generic condition $(1 - \alpha)\{2(\alpha\kappa - \kappa + \beta) + \beta(\kappa - \alpha - \beta)\} \neq 0$. If the generic condition is invalid, as shown above we can obtain normal forms of system (1.3) of other forms, which can be discussed similarly.

3. Versal unfoldings

In order to give a versal unfolding of system (1.3), in what follows we consider the 3-jet of the normal form (2.13)

$$\begin{cases} \dfrac{dx}{dt} = x\{\alpha x + (\alpha - 1)y + \tilde{a}_{20}x^2\}, \\ \dfrac{dy}{dt} = y\{(\kappa - \beta)x - \beta y\} \end{cases} \tag{3.1}$$

near the origin as the principal system [3], which is denoted by V_0. More generally, let $\mathcal{LV}(x)$ be the space of germs at the point $x = (x_1, x_2) \in \mathbf{R}^2$ of vector fields in the family of GLV systems and, fixed a neighborhood U_0 of the origin in $\mathbf{R}^2$, let

$$\mathcal{V} = \bigcup_{\xi \in U_0} \mathcal{LV}(\xi).$$

A germ $V_\xi \in \mathcal{V}$ at $\xi \in U_0$ defines a vector field of the GLV form

$$\frac{dx}{dt} = V(x), \quad x \in U_\xi, \tag{3.2}$$

where $U_\xi \subset U_0$ is a neighborhood of ξ.

Obviously, system V_0 is at least of codimension 2. Its versal unfolding of exact codimension 2 is the most fundamental and simplest situation. In order to give such a versal unfolding for V_0 in $\mathcal{V}$, we first need to describe the class of germs which have the same singularity as V_0. Actually, this class is

$$S = \{V_\xi \in \mathcal{V} \mid V_\xi \text{ satisfies } (H_1), (H_1), (H_3)\},$$

where

(H_1) the linearization of $V_\xi(x)$ at $x = \xi$ is $\left[\begin{smallmatrix} 0 & 0 \\ 0 & 0 \end{smallmatrix}\right]$;
(H_2) the coefficients of the terms of degree 2 in the expansion (2.1) of $V_\xi(x)$ satisfy

$$a_{ij}b_{ij}(a_{ij} - b_{ij})(a_{10}b_{01} - a_{01}b_{10}) \neq 0, \quad i, j = 0, 1, \ i \neq j;$$

(H_3) the coefficients of the terms of degree 3 in the expansion (2.1) of $V_\xi(x)$ are not all equal to 0.

In fact, without (H_2) additional degeneracy will be caused as explained after the proof of Lemma 1. Under (H_2) the coefficients of (2.1) are out of $\mathcal{Z}$ as shown in (2.12), so hypothesis (H_3) guarantees that (2.1) can be reduced surely to a normal form as in Lemma 1. Being a non-degeneracy condition, (H_2) together with (H_3) is generic in order to achieve an unfolding of codimension 2. Actually, we will prove that S forms a local submanifold of codimension 2 near V_0 in $\mathcal{V}$.

Lemma 2. *The set S is a smooth submanifold of codimension 2 near V_0 in $\mathcal{V}$.*

Proof. Let $J^k = \{j^k V_\xi \mid V_\xi \in \mathcal{V}\}$, where $k \in \mathbf{Z}^+$ and $j^k V_\xi$ is the k-jet of V_ξ at ξ, which corresponds to a truncated polynomial system of degree k. A natural projection $\pi_k : \mathcal{V} \to J^k$ can be defined by

$$V_\xi \mapsto (V(\xi), DV(\xi), \ldots, D^k V(\xi)),$$

where V is defined in (3.2) and $D^kV(\xi)$ is the kth order derivative of V at $x=\xi$. Note that $V(\xi)\equiv 0$ since $\mathcal{V}$ is in the family of GLV systems.

First of all, we prove that $\pi_1(S)$ constructs a smooth submanifold of codimension 2 near $\pi_1(V_0)$ in J^1. By the definition of S, we have

$$\pi_1(S)=\left\{\big(0, DV(\xi)\big) \;\Big|\; \frac{\partial V_1(\xi)}{\partial x_1}=\frac{\partial V_2(\xi)}{\partial x_2}=0\right\}, \tag{3.3}$$

where V_1 and V_2 are components of V. The structure of the submanifold for $\pi_1(S)$ is observed from the projection π_1 to a finite-dimensional Euclidean space. The two equalities in (3.3) confine the submanifold $\pi_1(S)$ to be of codimension 2 near $\pi_1(V_0)$ in J^1.

Next, we claim that for each $k\geqslant 2$ the set $\pi_k(S)$ is also a smooth submanifold of codimension 2 near $\pi_k(V_0)$ in J^k. The structure of the submanifold for $\pi_k(S)$ is observed similarly to the last step. Define a projection $\pi_{k1}: J^k\to J^1$ such that

$$\big(V(\xi), DV(\xi),\dots,D^kV(\xi)\big)\mapsto \big(V(\xi), DV(\xi)\big),$$

which is clearly a regular submersion. Hence, the map π_{k1} intersects $\pi_1(S)\subset J^1$ transversally. By Theorem 3.3 in [12] (p. 22), $\pi_{k1}^{-1}(\pi_1(S))$ is a smooth submanifold in J^k and the codimension of $\pi_{k1}^{-1}(\pi_1(S))$ in J^k is the same as the codimension of $\pi_1(S)$ in J^1, i.e.,

$$\operatorname{codim}\pi_{k1}^{-1}\big(\pi_1(S)\big)=\operatorname{codim}\pi_1(S)=2, \tag{3.4}$$

as shown in the last paragraph. On the other hand, $\pi_k(S)\subset\pi_{k1}^{-1}(\pi_1(S))$. Actually, $\pi_k(S)$ consists of those in $\pi_{k1}^{-1}(\pi_1(S))$ with restrictions (H_2) and (H_3). Furthermore, $\pi_k(S)$ is an open subset of $\pi_{k1}^{-1}(\pi_1(S))$ near $\pi_k(V_0)$ because of the strict inequalities (H_2) and (H_3). It follows from (3.4) that in J^k,

$$\operatorname{codim}\pi_k(S)=2. \tag{3.5}$$

Since π_k is a smooth submersion from $\mathcal{V}$ to J^k, we know that π_k intersects $\pi_k(S)\subset J^k$ transversally. As above, Theorem 3.3 in [12] also implies that $S=\pi_k^{-1}(\pi_k(S))$ is a smooth manifold in $\mathcal{V}$ and

$$\operatorname{codim}S=\operatorname{codim}\pi_k^{-1}\big(\pi_k(S)\big)=\operatorname{codim}\pi_k(S)=2$$

by (3.5). It means that S is a smooth submanifold of codimension 2 in $\mathcal{V}$. □

By Lemma 2, a versal unfolding of (2.13) has at least two unfolding parameters. Having the GLV form, a natural unfolding of system (2.13) near the origin is

$$\begin{cases} \dfrac{dx}{dt}=x\big\{\mu_1+\alpha x+(\alpha-1)y+\tilde a_{20}x^2\big\}:=X(x,y,\mu),\\[2mm] \dfrac{dy}{dt}=y\big\{\mu_2+(\kappa-\beta)x-\beta y\big\}:=Y(x,y,\mu),\end{cases} \tag{3.6}$$

where $\mu=(\mu_1,\mu_2)$ denotes the tuple of the unfolding parameters near $(0,0)$ and the condition

$$(\alpha-1)(\kappa-\beta)(\kappa-\alpha-\beta)(1-\alpha-\beta)(\alpha\kappa+\beta-\kappa)\tilde a_{20}\neq 0 \tag{3.7}$$

is required by the non-degeneracy conditions (H_2) and (H_3).

Now we can state and prove the main result of this section.

Theorem 3. *System* (3.6) *with* (3.7) *is a versal unfolding of system* (1.3).

Proof. Let $V(\mu) = (V_1(x, y, \mu_1, \mu_2), V_2(x, y, \mu_1, \mu_2))$ denote the family of vector fields in the form of (3.6). Clearly, $V(0) = V_0 \in S$. In order to prove the transversality of $V(\mu)$, define a map $g : \mathbf{R}^2 \to J^3$ by

$$\mu \mapsto \pi_3\big(V(\mu)\big) = \big(V(\mu), DV(\mu), D^2V(\mu), D^3V(\mu)\big).$$

It suffices to prove that g intersects $\pi_3(S) \subset J^3$ transversally at $\pi_3(V_0)$. Consider an open neighborhood $\mathcal{U}$ of $\mu = 0$. By condition (H_1) we have $DV(\mu) = 0$ at the intersection $g(\mathcal{U}) \cap \pi_3(S)$, i.e.,

$$\begin{cases} \dfrac{\partial}{\partial x} V_1(x, y, \mu_1, \mu_2) = \mu_1 + 2\alpha x + (\alpha - 1)y + 3\tilde{a}_{20}x^2 = 0, \\ \dfrac{\partial}{\partial y} V_2(x, y, \mu_1, \mu_2) = \mu_2 + (\kappa - \beta)x - 2\beta y = 0 \end{cases} \tag{3.8}$$

as in (3.3). Furthermore, the Jacobian matrix of g at $\mu = 0$ contains a sub-matrix

$$\begin{bmatrix} \frac{\partial}{\partial \mu_1}(\frac{\partial V_1}{\partial x}) & \frac{\partial}{\partial \mu_2}(\frac{\partial V_1}{\partial x}) \\ \frac{\partial}{\partial \mu_1}(\frac{\partial V_2}{\partial y}) & \frac{\partial}{\partial \mu_2}(\frac{\partial V_2}{\partial y}) \end{bmatrix}_{\mu=0} = \begin{bmatrix} 1 & 0 \\ 0 & 1 \end{bmatrix}, \tag{3.9}$$

which has rank 2. Therefore, the Jacobian matrix of g is of full rank, implying the transversality of g.

Furthermore, we can show that a general versal unfolding of (1.3), i.e.,

$$\begin{cases} \dfrac{dx}{dt} = x\big\{\mu_1 + \alpha x + (\alpha - 1)y - \alpha x^2 - \alpha xy + \mu_3 y^2\big\}, \\ \dfrac{dy}{dt} = y\big\{\mu_2 + (\kappa - \beta)x - \beta y + \mu_4 x^2 + \mu_5 xy + \mu_6 y^2\big\} \end{cases} \tag{3.10}$$

can be reduced to system (3.6) by a series of equivalent transformations. Let $\mu = (\mu_1, \mu_2, \mu_3, \mu_4, \mu_5, \mu_6)$. Consider the transformation

$$x = \tilde{x}(1 + w_1\tilde{x} + w_2\tilde{y}), \qquad y = \tilde{y}(1 + w_3\tilde{x} + w_4\tilde{y}), \qquad dt = (1 + w_5\tilde{x} + w_6\tilde{y})\,d\tilde{t}, \tag{3.11}$$

where $w_2 = -\mu_3/\beta - (\alpha - 1)\mu_6/\beta^2 + O(|\mu|^2)$, $w_4 = 0$, $w_6 = \mu_6/\beta$ and

$$\begin{aligned} w_1 = {} & \big\{\alpha\big(\beta^2 - \beta\kappa - \beta - \kappa\alpha + \kappa\big)/\big((1 - \alpha)\big(2\kappa - 2\kappa\alpha - 2\beta + \beta^2 - \beta\kappa + \alpha\beta\big)\big)\big\} \\ & + \big\{\big(3\beta^2 - 3\beta\kappa + \alpha\beta - 2\beta - 2\kappa\alpha + 2\kappa\big)(-\kappa + \beta)\alpha^2\beta/\big((\alpha - 1)\big(-2\kappa\alpha + \alpha\beta + 2\kappa \\ & + \beta^2 - 2\beta - \beta\kappa\big)^3\big)\big\}\mu_1 - \big\{\big(\beta^3 - 2\beta^2\kappa + \alpha^2\beta - 2\alpha\beta + \beta\kappa^2 - 2\kappa\alpha^2 + 2\kappa\alpha\big) \\ & /\big(\beta(\alpha - 1)\big(\alpha\beta - 2\kappa\alpha + 2\kappa + \beta^2 - 2\beta - \beta\kappa\big)\big)\big\}\mu_3 + \big\{(\alpha - 1)/\big(2\kappa - 2\kappa\alpha + \alpha\beta \\ & + \beta^2 - 2\beta - \beta\kappa\big)\big\}\mu_4 + \big\{(\beta - \alpha - \kappa)/\big(2\kappa - 2\kappa\alpha + \alpha\beta + \beta^2 - 2\beta - \beta\kappa\big)\big\}\mu_5 \\ & - \big\{(2\kappa - 2\kappa\alpha - 2\beta + \alpha\beta)\big(\beta^2 - \alpha - \alpha\beta - \beta\kappa + \alpha^2\big) \\ & /\big(\beta^2(\alpha - 1)\big(2\kappa - 2\kappa\alpha + \alpha\beta + \beta^2 - 2\beta - \beta\kappa\big)\big)\big\}\mu_6 + O\big(|\mu|^2\big), \end{aligned}$$

$$\begin{aligned}
w_3 = {} & \big\{(\kappa-\beta)\alpha\beta/\big((\alpha-1)\big(\alpha\beta-2\kappa\alpha+2\kappa+\beta^2-2\beta-\beta\kappa\big)\big)\big\} - \big\{\big(3\beta^2-3\beta\kappa+\alpha\beta-2\beta \\
& -2\kappa\alpha+2\kappa\big)(\beta-\kappa)\alpha^2\beta^2/\big((\alpha-1)^2\big(2\kappa-2\kappa\alpha+\alpha\beta+\beta^2-2\beta-\beta\kappa\big)^3\big)\big\}\mu_1 \\
& + \big\{(\kappa-\beta)\big(\beta^2+2\beta-\beta\kappa-\alpha\beta+2\kappa\alpha-2\kappa\big)/\big(\beta(\alpha-1)\big(\alpha\beta-2\kappa\alpha \\
& +2\kappa+\beta^2-2\beta-\beta\kappa\big)\big)\big\}\mu_3 - \big\{\beta/\big(\alpha\beta-2\kappa\alpha+2\kappa+\beta^2-2\beta-\beta\kappa\big)\big\}\mu_4 \\
& + \big\{2(\beta-\kappa)/\big(2\kappa-2\kappa\alpha+\alpha\beta+\beta^2-2\beta-\beta\kappa\big)\big\}\mu_5 \\
& - \big\{(-\kappa+\beta)\big(2\alpha\beta^2-3\beta^2+3\alpha\beta-3\beta\kappa\alpha+3\beta\kappa-\alpha^2\beta-2\beta+2\kappa\alpha^2-4\kappa\alpha+2\kappa\big) \\
& /\big(\beta^2(\alpha-1)\big(-2\kappa\alpha+\alpha\beta+2\kappa+\beta^2-2\beta-\beta\kappa\big)\big)\big\}\mu_6 + O\big(|\mu|^2\big), \\
w_5 = {} & \big\{\alpha(\alpha+\beta-1)(\beta-\kappa)/\big((\alpha-1)\big(-2\kappa\alpha+\alpha\beta+2\kappa+\beta^2-2\beta-\beta\kappa\big)\big)\big\} \\
& + \big\{\beta\alpha^2(\alpha+\beta-1)(\beta-\kappa)\big(3\beta^2-3\beta\kappa+\alpha\beta-2\beta-2\kappa\alpha+2\kappa\big) \\
& /\big((\alpha-1)^2\big(\alpha\beta-2\kappa\alpha+2\kappa+\beta^2-2\beta-\beta\kappa\big)^3\big)\big\}\mu_1 \\
& + \big\{(\beta-\kappa)(\beta-\kappa+\alpha)/\big((\alpha-1)\big(\alpha\beta-2\kappa\alpha+2\kappa+\beta^2-2\beta-\beta\kappa\big)\big)\big\}\mu_3 \\
& + \big\{(\alpha-1+\beta)/\big(\alpha\beta-2\kappa\alpha+2\kappa+\beta^2-2\beta-\beta\kappa\big)\big\}\mu_4 \\
& - \big\{(\beta-\kappa+\alpha)/\big(\alpha\beta-2\kappa\alpha+2\kappa+\beta^2-2\beta-\beta\kappa\big)\big\}\mu_5 \\
& + \big\{(\beta-\kappa)\big(\alpha\beta-2\beta+\alpha^2-\alpha+2\kappa-2\kappa\alpha\big) \\
& /\big(\beta(\alpha-1)\big(\alpha\beta-2\kappa\alpha+2\kappa+\beta^2-2\beta-\beta\kappa\big)\big)\big\}\mu_6 + O\big(|\mu|^2\big).
\end{aligned}$$

As in (2.3), the transformation (3.11) preserves the structure of GLV systems and changes system (3.10) into

$$\begin{cases} \dfrac{d\tilde{x}}{d\tilde{t}} = \tilde{x}\big\{\mu_1 + \big(\alpha+\epsilon_1(\mu)\big)\tilde{x} + \big(\alpha-1+\epsilon_2(\mu)\big)\tilde{y} + \hat{a}_{20}(\mu)\tilde{x}^2\big\}, \\ \dfrac{d\tilde{y}}{d\tilde{t}} = \tilde{y}\big\{\mu_2 + \big(\kappa-\beta+\epsilon_3(\mu)\big)\tilde{x} + \big(-\beta+\epsilon_4(\mu)\big)\tilde{y}\big\}, \end{cases} \tag{3.12}$$

where $\epsilon_1(\mu) = (w_5 - w_1)\mu_1$, $\epsilon_2(\mu) = w_6\mu_1 - w_2\mu_2$, $\epsilon_3(\mu) = -w_3\mu_1 + w_5\mu_2$, $\epsilon_4(\mu) = (w_6 - w_4)\mu_2$, $\hat{a}_{20}(\mu) = \tilde{a}_{20} + O(|\mu|)$ and $\tilde{a}_{20}$ is given in (2.14). In order to reduce (3.12) to the same form as in (3.6), we use the change of variables

$$\bar{x} = \bar{a}\tilde{x}, \qquad \bar{y} = \bar{b}\tilde{y}, \qquad \bar{t} = \tilde{t}/\bar{c}, \tag{3.13}$$

where $\bar{a} = \alpha\hat{a}_{20}(\mu)/(\alpha+\epsilon_1(\mu))\tilde{a}_{20}$, $\bar{b} = \alpha^2(\alpha-1+\epsilon_2(\mu))\hat{a}_{20}(\mu)/(\alpha+\epsilon_1(\mu))^2(\alpha-1)\tilde{a}_{20}$ and $\bar{c} = \alpha^2\hat{a}_{20}(\mu)/(\alpha+\epsilon_1(\mu))^2\tilde{a}_{20}$, which transforms (3.12) into

$$\begin{cases} \dfrac{d\bar{x}}{d\bar{t}} = \bar{x}\big\{\bar{c}\mu_1 + \alpha\bar{x} + (\alpha-1)\bar{y} + \tilde{a}_{20}\bar{x}^2\big\}, \\ \dfrac{d\bar{y}}{d\bar{t}} = \bar{y}\left\{\bar{c}\mu_2 + \dfrac{\bar{c}(\kappa-\beta+\epsilon_3(\mu))}{\bar{a}}\bar{x} + \dfrac{\bar{c}(-\beta+\epsilon_4(\mu))}{\bar{b}}\bar{y}\right\}. \end{cases}$$

This system is clearly the same as (3.6) with the new parameters

$$\bar{\mu}_1 := \bar{c}\mu_1, \qquad \bar{\mu}_2 := \bar{c}\mu_2, \qquad \bar{\beta} := \frac{\bar{c}(\beta-\epsilon_4(\mu))}{\bar{b}}, \qquad \bar{\kappa} := \frac{\bar{c}(\kappa-\beta+\epsilon_3(\mu))}{\bar{a}} + \bar{\beta}.$$

Observe that $\bar{a} = (1 - \epsilon_1(\mu)/\alpha + O(|\mu|^2))(1 + O(|\mu|)) = 1 + O(|\mu|)$. Similarly, $\bar{b} = 1 + O(|\mu|)$ and $\bar{c} = 1 + O(|\mu|)$. Therefore, $\bar{\beta} = \beta + O(|\mu|)$ and $\bar{\kappa} - \bar{\beta} = \kappa - \beta + O(|\mu|)$. It implies that, as β and κ, the new parameters $\bar{\beta}$ and $\bar{\kappa}$ satisfy the non-degeneracy condition (3.7). Moreover, transformations (3.11) and (3.13) are both orientation-preserving homeomorphisms. Hence, system (3.6) is a versal unfolding of system (1.3). □

4. Equilibria

We first discuss the qualitative properties of equilibria for the versal unfolding (3.6). It has at most six equilibria in the first quadrant: (i) $O = (0,0)$, (ii) $B_0 = (0, \mu_2/\beta)$ (exists if $\mu_2 > 0$), (iii) $A_0 = (x_+, 0)$ (exists if $\mu_1 < 0$), (iv) $A_1 = (x_-, 0)$ (exists if $\tilde{a}_{20} < 0$), (v) $C_0 = (x_0, y_0)$ (exists if $\Theta_0 > 0$, $\Xi_0 > 0$), and (vi) $C_1 = (x_1, y_1)$ (exists if $\Theta_1 > 0$, $\Xi_1 > 0$), where

$$\Theta_0 = \frac{-\beta\mu_1 + (1-\alpha)\mu_2}{\alpha\kappa + \beta - \kappa},$$

$$\Xi_0 = \frac{(\beta - \kappa)\mu_1 + \alpha\mu_2}{\alpha\kappa + \beta - \kappa},$$

$$\Theta_1 = \frac{\alpha\kappa + \beta - \kappa}{-\beta\tilde{a}_{20}},$$

$$\Xi_1 = \frac{(\beta - \kappa)(\alpha\kappa + \beta - \kappa)}{\beta^2\tilde{a}_{20}},$$

$$x_+ = \frac{-\alpha + \sqrt{\alpha^2 - 4\tilde{a}_{20}\mu_1}}{2\tilde{a}_{20}} = -\frac{\mu_1}{\alpha} - \frac{\tilde{a}_{20}}{\alpha^3}\mu_1^2 + O\left(|\mu_1|^3\right),$$

$$x_- = \frac{-\alpha - \sqrt{\alpha^2 - 4\tilde{a}_{20}\mu_1}}{2\tilde{a}_{20}} = -\frac{\alpha}{\tilde{a}_{20}} + \frac{1}{\alpha}\mu_1 + O\left(|\mu_1|^2\right),$$

$$x_0 = \frac{-(\alpha\kappa + \beta - \kappa) \mp \sqrt{(\alpha\kappa + \beta - \kappa)^2 - 4\tilde{a}_{20}\beta^2\mu_1 - 4\tilde{a}_{20}\beta(\alpha - 1)\mu_2}}{2\tilde{a}_{20}\beta} = \Theta_0 + O\left(|\mu|^2\right),$$

$$y_0 = \frac{\mu_2 + (\kappa - \beta)x_0}{\beta},$$

$$x_1 = \frac{-(\alpha\kappa + \beta - \kappa) \pm \sqrt{(\alpha\kappa + \beta - \kappa)^2 - 4\tilde{a}_{20}\beta^2\mu_1 - 4\tilde{a}_{20}\beta(\alpha - 1)\mu_2}}{2\tilde{a}_{20}\beta} = \Theta_1 + O\left(|\mu|^2\right),$$

$$y_1 = \frac{\mu_2 + (\kappa - \beta)x_1}{\beta}.$$

The sign $\mp$ in the expression of x_0 depends on whether $\alpha\kappa + \beta - \kappa < 0$ or > 0, and similarly in x_1. The last two equilibria lie in the interior of the first quadrant but the remaining four lie on its boundary.

Theorem 4. *System* (3.6) *has at most six equilibria*: O, B_0, A_0, A_1, C_0, *and* C_1 *in the first quadrant as defined above.*

(i) O *is a node* (*resp. saddle*) *when* $\mu_1\mu_2 > 0$ (*resp.* < 0).
(ii) B_0 *is a stable node* (*resp. saddle*) *when* $\mu_1 - ((1-\alpha)/\beta)\mu_2 < 0$ (*resp.* > 0).
(iii) A_0 *is an unstable node* (*resp. saddle*) *when* $\mu_2 - ((\kappa - \beta)/\alpha)\mu_1 > 0$ (*resp.* < 0).
(iv) A_1 *is a stable node* (*resp. saddle*) *when* $\beta - \kappa > 0$ (*resp.* < 0).
(v) C_0 *is either a saddle when* $\alpha\kappa - \kappa + \beta > 0$ *or a node* (*or focus*) *when* $\alpha\kappa - \kappa + \beta < 0$.
(vi) C_1 *is either a saddle when* $(\alpha\kappa - \kappa + \beta)(\kappa - \beta) < 0$ *or a node* (*or focus*) *when* $(\alpha\kappa - \kappa + \beta)(\kappa - \beta) > 0$.

Moreover, O, A_0 and B_0 are saddle-nodes when μ lies on the μ_1-(or μ_2-) axis and on the curves

$$\mathcal{Q}_{A_0C_0} := \left\{(\mu_1, \mu_2) \;\middle|\; \mu_2 = \frac{\kappa-\beta}{\alpha}\mu_1 + O\big(|\mu_1|^2\big),\ \mu_1 < 0\right\},$$
$$\mathcal{Q}_{B_0C_0} := \left\{(\mu_1, \mu_2) \;\middle|\; \mu_2 = \frac{\beta}{1-\alpha}\mu_1,\ \mu_2 > 0\right\},$$

respectively, all of which are transcritical bifurcation curves. C_0 is a stable weak focus with multiplicity 1 when μ lies on the Hopf bifurcation curve

$$\mathcal{Q}_H := \left\{(\mu_1, \mu_2) \;\middle|\; \mu_2 = \frac{\beta(\kappa-\alpha-\beta)}{\alpha(\alpha+\beta-1)}\mu_1 + O\big(|\mu_1|^2\big),\ \alpha\kappa-\kappa+\beta < 0,\ \Theta_0 > 0,\ \Xi_0 > 0\right\},$$

and a unique stable limit cycle arises when $\mu_2 - \beta(\kappa-\alpha-\beta)\mu_1/(\alpha(\alpha+\beta-1)) > 0$ (resp. < 0) is small for $\alpha+\beta-1 > 0$ (resp. < 0).

Proof. (i) It is easy to see that $O = (0,0)$ is a node (resp. saddle) when $\mu_1\mu_2 > 0$ (resp. < 0). In particular, O is an unstable (resp. stable) node if both $\mu_1 > 0$ and $\mu_2 > 0$ (resp. both $\mu_1 < 0$ and $\mu_2 < 0$). In the case that $\mu_1 = 0$ and $\mu_2 \neq 0$ or $\mu_1 \neq 0$ and $\mu_2 = 0$, the equilibrium O is degenerate. In the first case, from $Y(x, y, \mu) = 0$ in (3.6) we know that the branch passing through the origin is the curve $y = \varphi(x, \mu) = 0$. Thus, we consider zeros of the function

$$X\big(x, \varphi(x,\mu), \mu\big) = \mu_1 x + \alpha x^2 + \tilde{a}_{20}x^3 \tag{4.1}$$

for bifurcations of equilibria, where $X(x, y, \mu)$ is also defined in (3.6). As in [10] (Section 3.4) we know that O is a saddle-node when $\mu_1 = 0$ and a transcritical bifurcation occurs in system (3.6) when $\mu_2 \neq 0$ and μ_1 passes through 0. Actually, the equilibrium A_0 is bifurcated from O as $\mu_1 \neq 0$ but it does not lie in the first quadrant as $\mu_1 > 0$. In the other case, i.e., $\mu_1 \neq 0$ and $\mu_2 = 0$, we solve for $x = \phi(y, \mu) = 0$ from $X(x, y, \mu) = 0$ and discuss zeros of the function

$$Y\big(\phi(y,\mu), y, \mu\big) = \mu_2 y - \beta y^2. \tag{4.2}$$

Similarly, we know that O is a saddle-node and the equilibrium B_0 arises from a transcritical bifurcation in system (3.6) near O.

(ii) The same phenomenon also happens at $B_0 = (0, \mu_2/\beta)$, which exists in the first quadrant only when $\mu_2 > 0$. In fact, the linearization of system (3.6) at B_0 has eigenvalues $\mu_1 - ((1-\alpha)/\beta)\mu_2$ and $-\mu_2$. Discussion on the signs of eigenvalues gives the properties of B_0. When $\mu_1 - ((1-\alpha)/\beta)\mu_2$ is near 0, as in (4.1), we similarly derive from (3.6) a function

$$X_1(x,\mu) = \big(\mu_1 - (1-\alpha)\mu_2/\beta\big)x + (\alpha\kappa+\beta-\kappa)x^2/\beta + \tilde{a}_{20}x^3.$$

The dependence of its zeros upon μ gives the bifurcations of equilibria for system (3.6). From this function we know that B_0 is a saddle-node when $\mu_1 = ((1-\alpha)/\beta)\mu_2$ and the equilibrium C_0 arises from a transcritical bifurcation in system (3.6) near B_0.

(iii) Similarly, $A_0 = (x_+, 0)$ exists in the first quadrant only if $\mu_1 < 0$. The linearization of system (3.6) at A_0 has eigenvalues

$$\lambda_{01} = \frac{(-\alpha + \sqrt{\alpha^2 - 4\tilde{a}_{20}\mu_1})\sqrt{\alpha^2 - 4\tilde{a}_{20}\mu_1}}{2\tilde{a}_{20}} = -\mu_1 + O\big(|\mu_1|^2\big),$$
$$\lambda_{02} = \mu_2 + \frac{(\kappa-\beta)(-\alpha + \sqrt{\alpha^2 - 4\tilde{a}_{20}\mu_1})}{2\tilde{a}_{20}} = \mu_2 - \frac{\kappa-\beta}{\alpha}\mu_1 + O\big(|\mu_1|^2\big).$$

Discussion on the signs of λ_{01} and λ_{02} gives the properties of A_0. When $\mu_2-((\kappa-\beta)/\alpha)\mu_1$ is near 0, as in (4.2), we similarly derive from (3.6) a function

$$Y_1(y,\mu)=\big(\mu_2-(\kappa-\beta)\mu_1/\alpha+O\big(|\mu_1|^2\big)\big)y-\big((\alpha\kappa+\beta-\kappa)/\alpha\big)y^2+O\big(|y|^3\big).$$

The dependence of its zeros upon μ yields the bifurcations of equilibria for system (3.6). From this function we know that A_0 is a saddle-node when $\mu_2=((\kappa-\beta)/\alpha)\mu_1+O(|\mu_1|^2)$ and the equilibrium C_0 arises from a transcritical bifurcation in system (3.6) near A_0.

(iv) $A_1=(x_-,0)$ is a simple equilibrium which exists in the first quadrant only when $\tilde{a}_{20}<0$. More precisely, the linearization of system (3.6) at A_1 has eigenvalues

$$\lambda_1=\frac{(\alpha+\sqrt{\alpha^2-4\tilde{a}_{20}\mu_1})\sqrt{\alpha^2-4\tilde{a}_{20}\mu_1}}{2\tilde{a}_{20}}=\frac{\alpha^2}{\tilde{a}_{20}}+O\big(|\mu_1|\big),$$
$$\lambda_2=\mu_2+\frac{(\kappa-\beta)(-\alpha-\sqrt{\alpha^2-4\tilde{a}_{20}\mu_1})}{2\tilde{a}_{20}}=\frac{(\beta-\kappa)\alpha}{\tilde{a}_{20}}+O\big(|\mu|\big).$$

None of them is zero for small $|\mu|$ because of the requirement (3.7). Since $\beta\neq\kappa$, discussion on the signs of λ_1 and λ_2 gives the properties of A_1. We see that A_1 is a stable node (or saddle) when $\beta-\kappa>0$ (or <0).

(v) Consider $C_0=(x_0,y_0)$, which exists in the interior of the first quadrant only if $\Theta_0>0$ and $\Xi_0>0$. The linearization of system (3.6) at C_0 has trace and determinant

$$T_{C_0}=\frac{\beta(\kappa-\alpha-\beta)\mu_1-\alpha(\alpha+\beta-1)\mu_2}{\alpha\kappa-\kappa+\beta}+O\big(|\mu|^2\big),$$
$$D_{C_0}=-\frac{(\mu_2\alpha-\mu_2+\mu_1\beta)(-\mu_1\beta+\kappa\mu_1-\alpha\mu_2)}{\alpha\kappa-\kappa+\beta}+O\big(|\mu|^3\big).$$

Thus C_0 is either a saddle when $D_{C_0}<0$ or a node (or focus) when $D_{C_0}>0$. In particular, when C_0 is a node (or focus) it is stable (resp. unstable) when $T_{C_0}<0$ (resp. >0); i.e., $(\beta(\kappa-\alpha-\beta)\mu_1-\alpha(\alpha+\beta-1)\mu_2)/(\alpha\kappa-\kappa+\beta)<0$ (resp. >0). If $T_{C_0}=0$, i.e., $\mu_2=(\beta(\kappa-\alpha-\beta)/\alpha(\alpha+\beta-1))\mu_1+O(|\mu_1|^2)$, and $T_{C_0}^2-4D_{C_0}<0$, i.e., $\alpha\kappa-\kappa+\beta<0$, a Hopf bifurcation may occur at C_0. Compute the first Liapunov value

$$L_1=\frac{1}{\mu_2^2}\left\{\frac{3\tilde{a}_{20}\beta^2(\alpha-1)(\kappa-\alpha-\beta)^2}{16\alpha^2(\kappa-\beta)(\alpha\kappa+\beta-\kappa)}+O\big(|\mu|\big)\right\}\neq 0 \tag{4.3}$$

by (3.7). It implies that C_0 is a weak focus with multiplicity 1. Note that the inequality $\alpha\kappa-\kappa+\beta<0$ implies that $\beta<\kappa$ and $\alpha<1$. Therefore,

$$\tilde{a}_{20}<0. \tag{4.4}$$

In fact, when $\kappa<\alpha+\beta<1$ (resp. $1<\alpha+\beta<\kappa$) we have $\partial\tilde{a}_{20}/\partial\kappa>0$ (resp. <0). The monotonicity in κ implies that $\tilde{a}_{20}<\alpha(\alpha-2)/2(1-\alpha)<0$ (resp. $\tilde{a}_{20}<\alpha/(\alpha-1)<0$) since $\kappa<\alpha+\beta$ (resp. $\kappa>\beta/(1-\alpha)$). In the remaining case, i.e., $\alpha+\beta<\min\{1,\kappa\}$, we consider the monotonicity of $\eta(\alpha,\beta,\kappa)$ and $\delta(\alpha,\beta,\kappa)$, the numerator and the denominator of $\tilde{a}_{20}$ respectively, in β. It is easy to see that $\partial\eta/\partial\beta<0$ and $\partial\delta/\partial\beta>0$. For $\kappa<1$, we have that $\delta<\alpha\kappa(\kappa-1)(\alpha-1)^2<0$ since $\beta<\kappa(1-\alpha)$. Therefore $\tilde{a}_{20}=\alpha^2(\kappa-\beta)(\alpha+\beta-1)/(-\delta)-\alpha<0$. For $\kappa>1$, similarly we can see that $\eta>\alpha(\kappa-1)(\alpha-1)^2>0$ and $\delta<(1-\kappa)(\alpha-1)^2<0$ since $\beta<1-\alpha$, implying that $\tilde{a}_{20}<0$. For $\kappa=1$, we calculate directly that $\tilde{a}_{20}=\alpha(2-\alpha-\beta)/(1-\alpha)(\beta-2)<0$. From (4.3) and (4.4) we see that $L_1<0$ and C_0 is stable. Thus, the Hopf bifurcation curve $\mathcal{Q}_H$ is well defined as in the statement of the theorem.

(vi) $C_1 = (x_1, y_1)$ is a simple equilibrium which exists in the first quadrant when $\Theta_1 > 0$, $\Xi_1 > 0$. We can compute the trace T_{C_1} and determinant D_{C_1} of the linearization of system (3.6) at C_1 as follows:

$$T_{C_1} = \frac{(\alpha\kappa - \kappa + \beta)(\kappa\beta - \beta^2 - \alpha\beta + 2\alpha\kappa - 2\kappa + 2\beta)}{\tilde{a}_{20}\beta^2} + O\left(|\mu|\right),$$

$$D_{C_1} = \frac{(\alpha\kappa - \kappa + \beta)^3(\kappa - \beta)}{\tilde{a}_{20}^2\beta^3} + O\left(|\mu|\right).$$

Thus C_1 is either a saddle when $D_{C_1} < 0$ or a node (or focus) when $D_{C_1} > 0$. More concretely, when C_1 is a node (or focus) it is stable (resp. unstable) when $T_{C_1} < 0$ (resp. > 0); i.e., $(\alpha\kappa - \kappa + \beta)(\kappa\beta - \beta^2 - \alpha\beta + 2\alpha\kappa - 2\kappa + 2\beta)/\tilde{a}_{20} < 0$ (resp. > 0). □

5. Limit cycles

As known in Section 4, the only possible equilibria in the interior of the first quadrant are C_0 and C_1. Thus limit cycles (if exist) surround either C_0 or C_1. In what follows we first prove that there is no cycle surrounding C_1. Then we discuss the cycles surrounding C_0 in the case

$$\alpha\kappa + \beta - \kappa < 0, \tag{5.1}$$

because this equilibrium is a saddle in the other case.

Theorem 5. *When $\beta < \kappa$, $\alpha\kappa + \beta - \kappa > 0$ and $\tilde{a}_{20} < 0$, system* (3.6) *has no closed orbits in the first quadrant.*

Proof. In this case the possible closed orbits surround the equilibrium C_1 since C_1 lies in the interior of the first quadrant and C_0 is a saddle if it exists. Note that the interval J between -3 and $-(\alpha\kappa + \beta - \kappa + \beta(\alpha + \beta - \kappa))/(\alpha\kappa + \beta - \kappa)$ is nonempty. In fact, the denominator of $\tilde{a}_{20}$ contains the factor $\delta_1(\alpha, \beta, \kappa) = 2(\alpha\kappa + \beta - \kappa) + \beta(\kappa - \alpha - \beta)$, which is nonzero by the non-degeneracy condition (3.7). It is easy to show that $-3 < -(\alpha\kappa + \beta - \kappa + \beta(\alpha + \beta - \kappa))/(\alpha\kappa + \beta - \kappa)$ (resp. $>$) if $\delta_1(\alpha, \beta, \kappa) > 0$ (resp. < 0). For arbitrarily chosen $\iota \in J$, consider a Dulac function

$$\mathcal{W}(x, y) := x^\iota y^{(\alpha - 2\beta - 1 + \iota(\alpha - 1))/\beta} \tag{5.2}$$

and discuss the divergence of the modified vector field $(\mathcal{W}X(x, y, \mu), \mathcal{W}Y(x, y, \mu))$. Assume that the system has a closed orbit γ in the first quadrant. Since the y-axis coincides with a union of orbits, the distance ρ between the y-axis and γ is a definite positive constant. Therefore, $\operatorname{div}(\mathcal{W}X, \mathcal{W}Y)$ has zeros in the region $\mathcal{S} = \{(x, y)\colon\ x > \rho/2,\ \ y > 0\}$. On the other hand,

$$\begin{aligned} \operatorname{div}(\mathcal{W}X, \mathcal{W}Y) &= \frac{\partial}{\partial x}\left(\mathcal{W}X(x, y, \mu)\right) + \frac{\partial}{\partial y}\left(\mathcal{W}Y(x, y, \mu)\right) \\ &= \mathcal{W}(x, y)\left\{(\iota + 1)\mu_1 + \left(\frac{\alpha - \beta - 1 + \alpha\iota - \iota}{\beta}\right)\mu_2 + \frac{K(\alpha, \beta, \kappa)}{\beta}x + (\iota + 3)\tilde{a}_{20}x^2\right\}, \end{aligned} \tag{5.3}$$

where $K(\alpha, \beta, \kappa) = \alpha\kappa + \beta - \kappa + \beta(\alpha + \beta - \kappa) + \iota(\alpha\kappa + \beta - \kappa)$. One can check that $K(\alpha, \beta, \kappa) < 0$ (resp. > 0) and $(\iota + 3)\tilde{a}_{20} < 0$ (resp. > 0) when $\delta_1(\alpha, \beta, \kappa) > 0$ (resp. < 0). Thus, when $\delta_1(\alpha, \beta, \kappa) > 0$ we have

$$\operatorname{div}(\mathcal{W}X, \mathcal{W}Y) < \mathcal{W}(x, y)\left\{\frac{K(\alpha, \beta, \kappa)}{\beta}\frac{\rho}{2} + (\iota + 3)\tilde{a}_{20}\left(\frac{\rho}{2}\right)^2 + O\left(|\mu|\right)\right\} < 0$$

in $\mathcal{S}$ for sufficiently small $|\mu|$. In the other case we can also prove that $\mathrm{div}(\mathcal{W}X, \mathcal{W}Y) > 0$. This contradicts the existence of zeros of the divergence in $\mathcal{S}$. The proof is completed. □

Next we discuss closed orbits around the equilibrium C_0. In the case of (5.1), by Theorem 4, a unique stable limit cycle can arise from a Hopf bifurcation at C_0 when parameters pass through the bifurcation curve $\mathcal{Q}_H$. Now we further discuss the existence and uniqueness of the cycle for parameters not close to the Hopf bifurcation value and prove that the cycle will disappear as a heteroclinic loop arises.

Theorem 6. *Suppose that α, β, κ satisfy* (5.1) *and $\alpha + \beta < 1$. Then system* (3.6) *has a closed orbit in the first quadrant for small (μ_1, μ_2) in the region*

$$\mathcal{S}_L := \left\{(\mu_1, \mu_2) \in \mathbf{R}^2 \;\middle|\; \mu_1 > 0,\ \mu_2 < \frac{\beta(\kappa - \alpha - \beta)}{\alpha(\alpha + \beta - 1)}\mu_1 + O\big(|\mu_1|^2\big)\right\},$$

which lies on the right half plane but below the Hopf bifurcation curve $\mathcal{Q}_H$.

This result will be proved by using the Poincaré–Bendixson Theorem. An observation at equilibria at infinity makes it more convenient for us to construct an outer boundary in the proof.

Lemma 7. *System* (3.6) *has two equilibria at infinity, I_x and I_y, in the first quadrant locating on the positive half x-axis and y-axis, respectively. Moreover, I_x is a stable* (*or unstable*) *node if $\tilde{a}_{20} > 0$* (*or* < 0). *I_y is degenerate with a saddle sector when $\alpha + \beta < 1$ and $\tilde{a}_{20} < 0$.*

Proof. With the Poincaré transformation $x = 1/z$, $y = u/z$ and a change of time $d\tau = dt/z^2$, system (3.6) is reduced to

$$\begin{cases} \dfrac{du}{d\tau} = -\tilde{a}_{20}u + (\kappa - \alpha - \beta)uz + (1 - \alpha - \beta)u^2 z + (\mu_2 - \mu_1)uz^2, \\ \dfrac{dz}{d\tau} = -\tilde{a}_{20}z - \alpha z^2 + (1 - \alpha)uz^2 - \mu_1 z^3. \end{cases} \tag{5.4}$$

On the u-axis system (5.4) has only one equilibrium $(0, 0)$, i.e., off the y-axis system (3.6) has exactly one equilibrium I_x at infinity in the first quadrant, locating on the positive half x-axis. Eigenvalues of (5.4) at $(0, 0)$ are both the same $-\tilde{a}_{20}$. Thus, the equilibrium is a stable (or unstable) node if $\tilde{a}_{20} > 0$ (or < 0).

With another Poincaré transformation $x = v/z$, $y = 1/z$ and the same change of time, system (3.6) is rewritten as

$$\begin{cases} \dfrac{dv}{d\tau} = (\alpha + \beta - 1)vz + \tilde{a}_{20}v^3 + (\alpha + \beta - \kappa)v^2 z + (\mu_1 - \mu_2)vz^2, \\ \dfrac{dz}{d\tau} = \beta z^2 + (\beta - \kappa)vz^2 - \mu_2 z^3. \end{cases} \tag{5.5}$$

Obviously, $I_0 = (0, 0)$ is a degenerate equilibrium of (5.5), i.e., system (3.6) has a degenerate equilibrium I_y at infinity on the positive y-axis. With the polar coordinates $v = r\cos\theta, z = r\sin\theta$, system (5.5) is reduced to

$$\frac{1}{r}\frac{dr}{d\theta} = \frac{H(\theta) + o(1)}{G(\theta) + o(1)} \quad \text{as } r \to 0,$$

where $G(\theta) = \sin^2\theta\cos\theta(1-\alpha)$, $H(\theta) = \beta\sin^3\theta + (\alpha+\beta-1)\sin\theta\cos^2\theta$. Function G has exactly two zeros 0 and $\pi/2$ in the first quadrant, which are both possible exceptional directions [23,28]. Obviously, the v-axis and z-axis each coincides with an orbit. We hope to know others except for these two. Clearly, $\theta_0 = \pi/2$ is a simple zero of G and satisfies $H(\pi/2) = \beta > 0$, $G'(\pi/2)H(\pi/2) = \beta(\alpha-1) < 0$. It follows that exact one orbit leaves I_0 in $\theta_0 = \pi/2$, by Theorem 6 in Chapter 5 of [23] (or Theorem 3.7 in Chapter 2 of [28]).

We have difficulties with the direction $\theta_0 = 0$ since it is a double zero of G and satisfies $H(0) = 0$ and $G'(0)H(0) = 0$. In such a situation no theorems in [23] and [28] are applicable. However, from (5.5) we see that $dz/dv < 0$ near I_0 in the interior of the first quadrant. By Lemma 4 in [24], no orbits connect with I_0 in $\theta_0 = 0$ in the interior. So the unique orbit, which approaches I_0, lies on the positive v-axis. □

Proof of Theorem 6. Under condition (5.1) we have $\beta < \kappa$, $\alpha < 1$. Moreover, $\tilde{a}_{20} < 0$ by (4.4). As defined in Theorem 4, the curves $\mathcal{Q}_{A_0C_0}$ and $\mathcal{Q}_{B_0C_0}$ lie in the third and first quadrant of the (μ_1, μ_2)-plane respectively. The inequalities $\Theta_0 > 0$ and $\Xi_0 > 0$ in the definition of the Hopf bifurcation curve $\mathcal{Q}_H$ imply that $\mathcal{Q}_H$ lies in the first, forth and third quadrant, respectively, when α, β, κ satisfy conditions $\kappa < \alpha+\beta < 1$, $\alpha+\beta < \min\{1,\kappa\}$ and $1 < \alpha+\beta < \kappa$. In our case, $\alpha+\beta < 1$, as stated in the theorem. Thus it suffices to discuss the case $\kappa < \alpha+\beta < 1$ and the case $\alpha+\beta < \min\{1,\kappa\}$.

In the first case, we prove the existence of closed orbits by the Poincaré–Bendixson Theorem [11] for (μ_1, μ_2) in the sub-regions

$$\mathcal{S}_L^1 := \left\{(\mu_1,\mu_2) \in \mathbf{R}^2 \;\middle|\; 0 < \mu_2 < \frac{\beta(\kappa-\alpha-\beta)}{\alpha(\alpha+\beta-1)}\mu_1 + O\big(|\mu_1|^2\big),\ \mu_1 > 0\right\}$$

and $\mathcal{S}_L^4$, the closure of the fourth quadrant.

For (μ_1, μ_2) in $\mathcal{S}_L^1$, by Theorem 4, system (3.6) has an unstable node $O = (0,0)$, two saddles $A_1 = (x_-, 0)$ and $B_0 = (0, \mu_2/\beta)$, and an unstable node or focus $C_0 = (x_0, y_0)$. Moreover, at infinity it has an unstable node I_x and a degenerate equilibrium I_y with a saddle sector, as shown in Lemma 7. System (3.6) has a vertical isocline $\mathcal{V}'$: $y = (\tilde{a}_{20}x^2 + \alpha x + \mu_1)/(1-\alpha)$ and a horizontal isocline $\mathcal{H}'$: $y = ((\kappa-\beta)/\beta)x + \mu_2/\beta$ uniquely in the interior of the first quadrant. Obviously, $\mathcal{V}'$ passes through A_1 and C_0 and intersects the y-axis at $D = (0, \mu_1/(1-\alpha))$, a point located above the equilibrium B_0 because

$$\mu_1 > \left(\frac{1-\alpha}{\beta}\right)\mu_2 \tag{5.6}$$

in $\mathcal{S}_L^1$, which follows the fact that $\beta(\kappa-\alpha-\beta)/(\alpha(\alpha+\beta-1)) < \beta/(1-\alpha)$, i.e., the curve $\mathcal{Q}_H$ lies below $\mathcal{Q}_{B_0C_0}$, under condition (5.1) and the assumption $\kappa < \alpha+\beta < 1$ for the first case. Similarly, $\mathcal{H}'$ passes through B_0 and C_0. We will show that the curve of the unstable manifold $W^u_{B_0}$ of B_0 goes around C_0 and intersects $\mathcal{H}'$ at a point E_* between B_0 and C_0 so that the arc $\widehat{B_0E_*}$ of this curve and the segment $\overline{E_*B_0}$ on $\mathcal{H}'$ compose the outer boundary for the application of the Poincaré–Bendixson Theorem.

Firstly, the saddle B_0 has its stable manifold $W^s_{B_0}$ on the y-axis and its unstable manifold $W^u_{B_0}$ with the slope $(\kappa-\beta)\mu_2/(\beta\mu_1 + (\alpha+\beta-1)\mu_2)$ at B_0, which is greater than 0 but less than $(\kappa-\beta)/\beta$ by (5.6). Thus, $W^u_{B_0}$ lies below $\mathcal{H}'$ and above the positive x-axis but cannot go through the segments $\overline{OA_1}$ and $\overline{OB_0}$ by the uniqueness of solutions and the qualitative properties of O and A_1. Moreover, $W^u_{B_0}$ cannot go back to intersect the open segment $\overline{B_0C_0}$ on $\mathcal{H}'$ because

$$\dot{x}|_{\mathcal{H}'} = xQ_1(x) \tag{5.7}$$

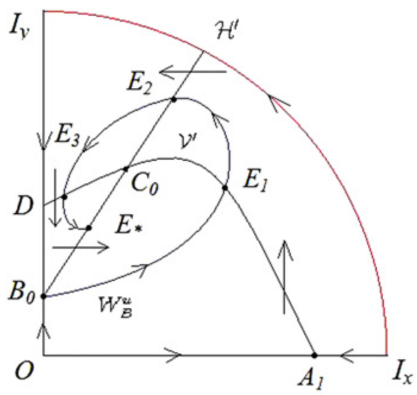

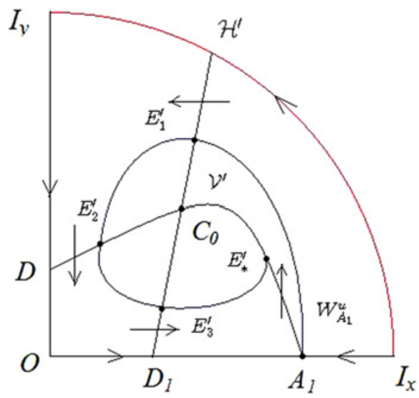

Fig. 1. Left: Outer boundary for $\mu \in \mathcal{S}_L^1$. Right: Outer boundary for $\mu \in \mathcal{S}_L^4$.

by (3.6) and the quadratic function

$$Q_1(x) = \tilde{a}_{20}x^2 + \big((\alpha\kappa + \beta - \kappa)/\beta\big)x + \mu_1 + \big((\alpha - 1)/\beta\big)\mu_2$$

is positive for $x \in (0, x_0)$. In fact, $\tilde{a}_{20} < 0$ by (4.4) and $Q_1(x)$ has its zeros at $x_1 < 0$ and $x_0 > 0$ by Theorem 4. Since C_0 is unstable, $W_{B_0}^u$ has to intersect with the arc of $\mathcal{V}'$ between A_1 and C_0 at a point E_1.

Secondly, on the parabola $\mathcal{V}'$ we have

$$\dot{y}|_{\mathcal{V}'} = yQ_2(x), \tag{5.8}$$

where the quadratic function

$$Q_2(x) = \big(-\beta\tilde{a}_{20}/(1-\alpha)\big)x^2 - \big((\alpha\kappa + \beta - \kappa)/(1-\alpha)\big)x + \mu_2 - \big(\beta/(1-\alpha)\big)\mu_1$$

is positive for $x > x_0$ because $\tilde{a}_{20} < 0$ and $Q_2(x)$ also has zeros at $x_1 < 0$ and $x_0 > 0$. Thus all orbits from the arc $\widehat{A_1C_0}$ of $\mathcal{V}'$ leave the region surrounded by $\overline{OA_1}$, $\widehat{A_1C_0}$, $\overline{C_0B_0}$ and $\overline{B_0O}$ by the convexity of the parabola. The repellency of the equilibrium I_x at infinity forces $W_{B_0}^u$ to intersect $\mathcal{H}'$ outside the segment $\overline{B_0C_0}$. Let E_2 denote the intersection point.

Obviously, $\dot{x} < 0$ at E_2 by (5.7), i.e., as an orbit the curve $W_{B_0}^u$ penetrates $\mathcal{H}'$ at E_2 from one side to the other. Thus, thirdly, such a curve will finally intersect $\mathcal{V}'$ again on the open arc $\widehat{C_0D}$ by the repellency of I_y and the uniqueness of solutions. We denote the intersection point by E_3. Similarly, we also know that $W_{B_0}^u$ penetrates $\mathcal{V}'$ at E_3 and enters the region surrounded by $\widehat{C_0D}$, $\overline{DB_0}$ and $\overline{B_0C_0}$ since $\dot{x} = 0$, $\dot{y} < 0$ at E_3 by (5.8) and the slope of $\mathcal{V}'$ at E_3 is a positive number. At last, the repellency of C_0 and B_0 forces $W_{B_0}^u$ to intersect $\mathcal{H}'$ again on the open segment $\overline{B_0C_0}$ of $\mathcal{H}'$ at a point E_*.

Thus, as shown in Fig. 1(left), the closed curve $B_0\widehat{E_1E_2E_3}E_* \cup \overline{E_*B_0}$ makes an outer boundary, from which no orbits leave the closed region surrounded by this closed curve. Since the equilibrium C_0 is unstable, the Poincaré–Bendixson Theorem ensures the existence of a closed orbit in this closed region.

For (μ_1, μ_2) in $\mathcal{S}_L^4$, by Theorem 4 and Lemma 7, system (3.6) has the same situation of equilibria as for (μ_1, μ_2) in $\mathcal{S}_L^1$, except B_0 disappears and O becomes a saddle. Moreover, in this case system (3.6) has the same vertical isocline $\mathcal{V}'$ and horizontal isocline $\mathcal{H}'$ as for (μ_1, μ_2) in $\mathcal{S}_L^1$. Similarly, $\mathcal{V}'$ passes through A_1 and C_0 and intersects the y-axis at the same point D as above, but $\mathcal{H}'$ passes through C_0 and intersects the positive x-axis at the point $D_1 = (-\mu_2/(\kappa - \beta), 0)$, which obviously lies on the left-hand side of A_1 for small $|\mu_2|$. We claim that the unstable manifold $W_{A_1}^u$ of A_1 goes around C_0 and intersects $\mathcal{V}'$ at a point E_*' between A_1 and C_0 so that the arc $\widehat{A_1E_*'}$ of $W_{A_1}^u$ and the arc $\widehat{E_*'A_1}$ of $\mathcal{V}'$ compose the outer boundary for application of the Poincaré–Bendixson Theorem.

Firstly, the saddle A_1 has its stable manifold $W^s_{A_1}$ on the x-axis and its unstable manifold $W^u_{A_1}$ with the slope $(\kappa+\alpha-\beta)/(\alpha-1)+O(|\mu|)<0$ at A_1. Note that the slope of $\mathcal{V}'$ at A_1 is $\alpha/(\alpha-1)+O(|\mu|)$ and $(\kappa+\alpha-\beta)/(\alpha-1)<\alpha/(\alpha-1)<0$. It follows that $W^u_{A_1}$ lies on the right-hand side of $\mathcal{V}'$ near A_1. By repellency of A_1, C_0 and I_x and the uniqueness of solutions, $W^u_{A_1}$ has to intersect either $\mathcal{H}'$ outside the closed segment $\overline{D_1C_0}$ or the open arc $\widehat{A_1C_0}$ of $\mathcal{V}'$. However, the second option is impossible because on the parabola $\mathcal{V}'$ we have $\dot{y}|_{\mathcal{V}'}=yQ_2(x)>0$ for $x>x_0$ by (5.8). Let E'_1 denote the intersection point for the first option.

Using the same arguments as in the case of $\mathcal{S}^1_L$, we know that $W^u_{A_1}$ penetrates $\mathcal{H}'$ at E'_1 from one side to the other because $\dot{x}=xQ_1(x)<0, \dot{y}=0$ at E'_1 by (5.7). After penetration, the repellency of I_y and C_0 forces $W^u_{A_1}$ to intersect $\mathcal{V}'$ again on the open arc $\widehat{C_0D}$. Let E'_2 denote this intersection point. Furthermore, as an orbit $W^u_{A_1}$ has to enter the region surrounded by $\widehat{C_0D}$, $\overline{DO}$, $\overline{OD_1}$ and $\overline{D_1C_0}$ because $\dot{x}=0, \dot{y}=yQ_2(x)<0$ at E'_2 by (5.8) and the slope of the parabola $\mathcal{V}'$ at this point is a positive number. For the same reason, the repellency of C_0 and O forces $W^u_{A_1}$ to intersect $\mathcal{H}'$ again at a point E'_3 on the segment $\overline{D_1C_0}$.

Finally, $\dot{x}=xQ_1(x)>0, \dot{y}=0$ at E'_3 by (5.7), which implies that $W^u_{A_1}$ enters the region surrounded by $\overline{C_0D_1}$, $\overline{D_1A_1}$ and the arc $\widehat{A_1C_0}$ of $\mathcal{V}'$. Therefore, the repellency of C_0 and A_1 also forces it to intersect $\mathcal{V}'$ again at a point E'_* on the arc $\widehat{A_1C_0}$. As shown in Fig. 1(right), the closed curve $A_1E'_1\widehat{E'_2}E'_3E'_*A_1$ makes an outer boundary, from which no orbits leave the surrounded closed region. The Poincaré–Bendixson Theorem implies the existence of a closed orbit in this closed region.

The discussion in the subcase when $\alpha+\beta<\min\{1,\kappa\}$ is totally a repetition of that for $\mu\in\mathcal{S}^4_L$ in the subcase when $\kappa<\alpha+\beta<1$. Similarly we obtain the existence of a closed orbit and the proof of the theorem is completed. □

We now study the uniqueness of the closed orbit given above. It suffices to discuss the uniqueness under condition (5.1) and the condition that $\Theta_0>0$, $\Xi_0>0$. These conditions guarantee that $C_0=(x_0,y_0)$ is not a saddle and $x_0>0, y_0>0$, respectively, as shown in Theorem 4 and in the proof of Theorem 6. Our strategy is to reduce system (3.6) to the form of a generalized Liénard system

$$\begin{cases}\dot{x}=\Phi(y)-F(x),\\ \dot{y}=-g(x)\end{cases}\tag{5.9}$$

and apply a known result (Theorem 1.1 in [16]) on the uniqueness of limit cycles, which is a modification of Z.-F. Zhang's Theorem in [27] as given in [7,8]. For this purpose, re-arrange terms in system (3.6) in the order of the powers of y, i.e.,

$$\begin{cases}\dot{x}=F_0(x)-F_1(x)y,\\ \dot{y}=G_1(x)y+G_2(x)y^2,\end{cases}\tag{5.10}$$

where $F_0(x)=x(\mu_1+\alpha x+\tilde{a}_{20}x^2)$, $F_1(x)=(1-\alpha)x$, $G_1(x)=\mu_2+(\kappa-\beta)x$ and $G_2(x)=-\beta$. Then, we need some transformations to eliminate terms containing the product xy in the first equation of (5.10) and lower the degree of the second one of (5.10) in y. The two transformations

$$x=x,\qquad \tilde{y}=F_0(x)-F_1(x)y,\tag{5.11}$$

and

$$x=x,\quad u=\tilde{y}\exp\left(\int_{x_0}^{x}E(w)\,dw\right),\qquad d\tilde{t}=\exp\left(-\int_{x_0}^{x}E(w)\,dw\right)dt,\tag{5.12}$$

where $E(x)=(G_2(x)-F'_1(x))/F_1(x)$, change system (5.10) into

$$\begin{cases} \dot{x} = u, \\ \dot{u} = -\Psi_0(x)\exp\left(\int\limits_{x_0}^{x} 2E(w)\,dw\right) - u\Psi_1(x)\exp\left(\int\limits_{x_0}^{x} E(w)\,dw\right), \end{cases} \tag{5.13}$$

where

$$\Psi_0(x) = F_0(x)\big\{F_1(x)G_1(x) + F_0(x)G_2(x)\big\}/F_1(x),$$
$$\Psi_1(x) = -F_0'(x) - G_1(x) + \big\{F_1'(x)F_0(x) - 2F_0(x)G_2(x)\big\}/F_1(x).$$

Obviously, the first equation of system (5.13) has the simplest form and the degree of the second equation is lowered by 1. Another transformation

$$x = x, \qquad v = u - F_0(x)\exp\left(\int\limits_{x_0}^{x} E(w)\,dw\right) + F_0(x_0) \tag{5.14}$$

changes system (5.13) further into

$$\begin{cases} \dot{x} = v + F_0(x)\exp\left(\int\limits_{x_0}^{x} E(w)\,dw\right) - F_0(x_0), \\ \dot{v} = \dfrac{F_1(x)G_1(x) + F_0(x)G_2(x)}{F_1(x)}\exp\left(\int\limits_{x_0}^{x} E(w)\,dw\right)\big(v - F_0(x_0)\big), \end{cases} \tag{5.15}$$

a form in which variables are separated in the first equation by addition and in the second equation by multiplication. Note that $F_0(x_0) = F_1(x_0)y_0 = (1-\alpha)x_0y_0 > 0$ because $\alpha < 1$ by (5.1), and that $v < F_0(x_0)$ because $F_1(x) = (1-\alpha)x > 0$ implies that $\tilde{y} < F_0(x)$. Therefore, $u - F_0(x)\exp(\int_{x_0}^{x} E(w)\,dw) + F_0(x_0) < F_0(x_0)$. So $1 - v/F_0(x_0) > 0$ and the transformation

$$\hat{x} = x, \qquad \hat{y} = \ln\left(1 - \frac{v}{F_0(x_0)}\right), \qquad d\hat{t} = -F_0(x_0)\,d\tilde{t} \tag{5.16}$$

can be applied to reduce system (5.15) to the form (5.9), where

$$\begin{cases} \Phi(y) = e^y - 1, \qquad F(x) = \dfrac{F_0(x)}{F_0(x_0)}\exp\left(\int\limits_{x_0}^{x} E(w)\,dw\right) - 1, \\ g(x) = \dfrac{F_1(x)G_1(x) + F_0(x)G_2(x)}{F_0(x_0)F_1(x)}\exp\left(\int\limits_{x_0}^{x} E(w)\,dw\right). \end{cases} \tag{5.17}$$

Theorem 8. *System* (3.6) *has at most one closed orbit in the interior of the first quadrant under condition* (5.1) *and the inequalities* $\alpha + \beta < 1$ *and*

$$\beta(\kappa - \alpha - \beta)\mu_1 + \alpha(1 - \alpha - \beta)\mu_2 < 0. \tag{5.18}$$

Moreover, the closed orbit is stable if it exists.

Proof. Clearly, transformations (5.11), (5.12), (5.14) and (5.16) are all one-to-one for $x > 0$ and $y > 0$, so it is equivalent to discuss the uniqueness of closed orbit of system (5.9) for $x > 0$. With those transformations, the coordinates of the equilibrium $C_0 = (x_0, y_0)$ of system (5.10) is translated into $(x_0, 0)$ for system (5.9). From (5.17), we calculate

$$f(x) := F'(x) = -\frac{(2\tilde{a}_{20}\alpha - 2\tilde{a}_{20} + \tilde{a}_{20}\beta)x^2 + \alpha(\alpha+\beta-1)x + \beta\mu_1}{F_0(x_0)(1-\alpha)} \exp\left(\int_{x_0}^{x} E(w)\,dw\right),$$

$$g(x) := \frac{Q_2(x)}{F_0(x_0)} \exp\left(\int_{x_0}^{x} E(w)\,dw\right),$$

where $Q_2(x)$ is defined in (5.8). Clearly, $\Phi'(y) = e^y > 0$ for all $y \in \mathbf{R}$ and $g(x_0) = 0$, $(x - x_0)g(x) > 0$ for $0 < x \neq x_0$ by the properties of $Q_2(x)$ as shown below (5.8). Thus conditions (i) and (ii) in Theorem 1.1 in [16] hold. In order to verify condition (iii), we calculate

$$f(x_0) = \left\{\frac{\beta(\kappa-\alpha-\beta)\mu_1 - \alpha(\alpha+\beta-1)\mu_2 + O(|\mu|^2)}{\alpha\kappa + \beta - \kappa}\right\} \exp\left(\int_{x_0}^{x} E(w)\,dw\right) > 0, \quad (5.19)$$

where the negativeness of the denominator and the numerator is guaranteed by (5.1) and (5.18). On the other hand,

$$\frac{d}{dx}\left(\frac{f(x)}{g(x)}\right) = \frac{h(x)}{Q_2^2(x)(\alpha-1)} \quad \text{for } 0 < x \neq x_0, \quad (5.20)$$

where

$$\begin{aligned} h(x) &= \tilde{a}_{20}\big(2\alpha\kappa + 2\beta - 2\kappa + \beta\kappa - \beta\alpha - \beta^2\big)x^2 \\ &\quad + 2\tilde{a}_{20}\big(2\beta\mu_1 + (\beta + 2\alpha - 2)\mu_2\big)x - \big(\beta(\kappa-\alpha-\beta)\mu_1 + \alpha(1-\alpha-\beta)\mu_2\big). \end{aligned}$$

Note that the coefficient of x^2 in $h(x)$ is equal to $\tilde{a}_{20}\delta(\alpha,\beta,\kappa)/(1-\alpha)$, where $\delta(\alpha,\beta,\kappa)$, the denominator of $\tilde{a}_{20}$, is less than 0 in the case when $\alpha + \beta < \min\{1, \kappa\}$ as defined and proved after (4.4) in the proof of Theorem 4. Since we assume in Theorem 8 that $\alpha + \beta < 1$, the other case is $\kappa < \alpha + \beta < 1$ by (3.7). In this case it is obvious that $\delta(\alpha,\beta,\kappa) < 0$ under (5.1). Moreover, $\tilde{a}_{20} < 0$ by (4.4) and $1 - \alpha > 0$ as implied by (5.1). Thus the coefficient of x^2 in the quadratic function $h(x)$ is positive. On the other hand, (5.18) implies that the discriminant Δ of $h(x)$ satisfies

$$\begin{aligned} \Delta &= 4\tilde{a}_{20}^2\big(2\beta\mu_1 + (\beta + 2\alpha - 2)\mu_2\big)^2 + 4\left(\frac{\tilde{a}_{20}\delta}{1-\alpha}\right)\big(\beta(\kappa-\alpha-\beta)\mu_1 + \alpha(1-\alpha-\beta)\mu_2\big) \\ &= 4\left(\frac{\tilde{a}_{20}\delta}{1-\alpha}\right)\big\{\beta(\kappa-\alpha-\beta)\mu_1 + \alpha(1-\alpha-\beta)\mu_2 + O\big(|\mu|^2\big)\big\} < 0. \end{aligned}$$

This implies that $h(x) > 0$ for all $x \in \mathbf{R}$, i.e., $(d/dx)(f(x)/g(x)) < 0$ for $0 < x \neq x_0$, by (5.20). Together with (5.19) it proves condition (iii) in Theorem 1.1 in [16]. Therefore, system (3.6) has at most one closed orbit which is hyperbolic if it exists. Furthermore, conditions (5.1) and (5.18) imply that the equilibrium C_0 is an unstable focus or node as shown in the proof of Theorem 4. Hence, the limit cycle is stable if it exists. □

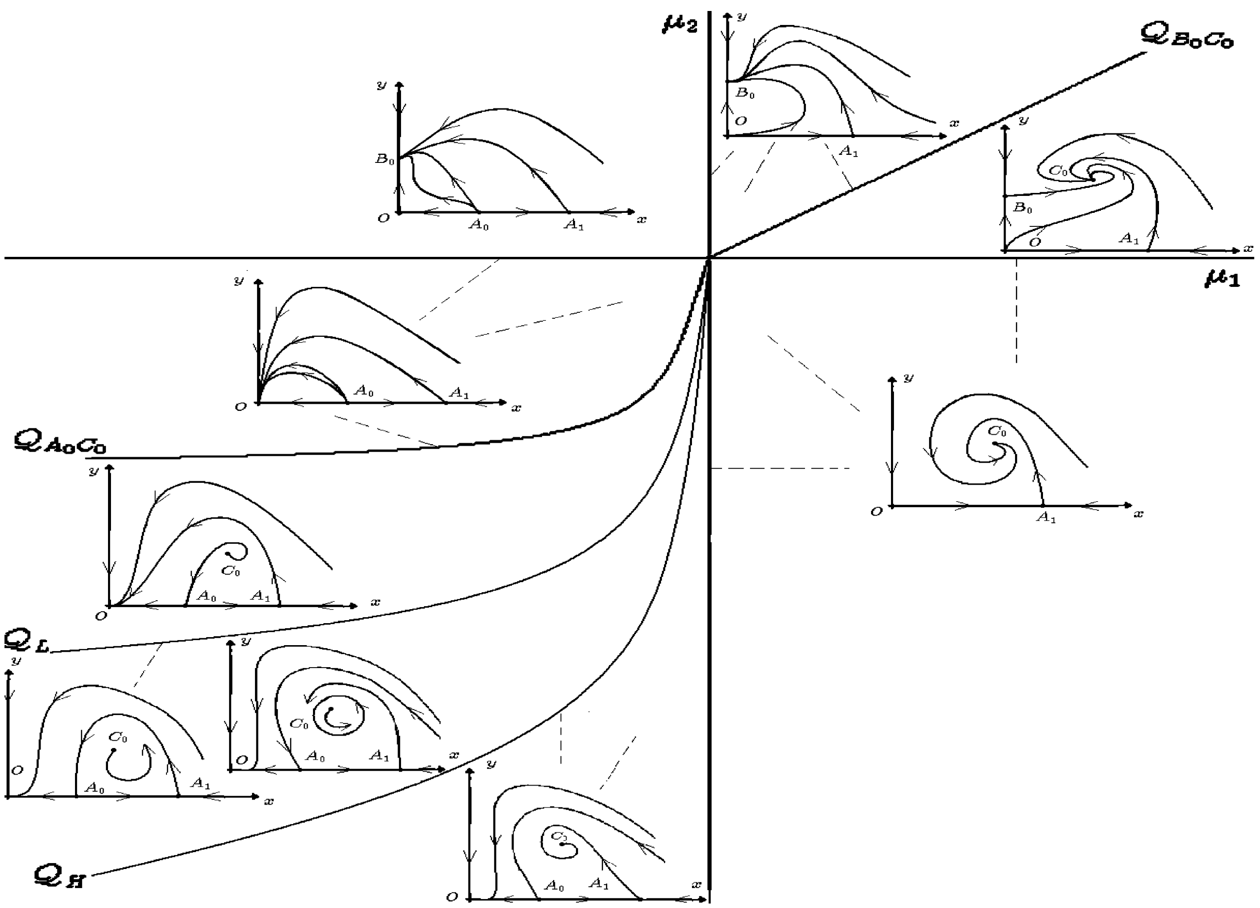

Fig. 2. Bifurcation diagram in case (C1) when $\beta < \kappa$, $\alpha < 1$, $\alpha\kappa + \beta - \kappa < 0$ and $1 < \alpha + \beta < \kappa$.

6. Heteroclinic loops

Notice that (5.18) describes a region below the line $\mu_2 = (\beta(\kappa - \alpha - \beta)/\alpha(\alpha + \beta - 1))\mu_1$ in the (μ_1, μ_2)-plane and the Hopf bifurcation curve $\mathcal{Q}_H$ is tangent to this line at the origin. Since exact one limit cycle can be produced from the Hopf bifurcation, we assure by Theorem 8 that in the region $\mathcal{S}_L$ system (3.6) has exact one limit cycle when $\alpha + \beta < 1$. From Theorem 4 we know that the slope of the curve $Q_{A_0C_0}$ is larger than that of the line under (5.1). Thus we also assure the uniqueness of a limit cycle in the subset of the third quadrant between the negative μ_2-axis and the curve $Q_{A_0C_0}$, as shown in Fig. 2, when $\alpha + \beta < 1$. If this limit cycle exists, it lies between the vertical lines ℓ_0: $x = x_+$ (resp. the positive y-axis) and ℓ_1: $x = x_-$ if $A_0 = (x_+, 0)$ exists (resp. not) in the first quadrant, because $\dot{x} = (\alpha - 1)x_+ y < 0$ on $\ell_0 \backslash \{A_0\}$ and $\dot{x} = (\alpha - 1)x_- y < 0$ on $\ell_1 \backslash \{A_1\}$.

Up to now, the existence of limit cycles remains unclear for (μ_1, μ_2) in the open subset $\mathcal{S}_L^3$ of the third quadrant between $\mathcal{Q}_{A_0C_0}$ and the negative μ_2-axis. In the other case, i.e., $1 < \alpha + \beta < \kappa$, which has not been dealt with previously, the Hopf bifurcation curve $\mathcal{Q}_H$ lies in $\mathcal{S}_L^3$ but the result of existence of limit cycles is also uncomplete in $\mathcal{S}_L^3$.

The following theorem gives a further answer.

Theorem 9. *Under condition* (5.1) *there exists a curve $\mathcal{Q}_L$ in the (μ_1, μ_2)-plane on which the limit cycle of system* (3.6) *arising from the Hopf bifurcation disappears, while a heteroclinic loop of* (3.6) *connecting A_0 with A_1 exists. The curve $\mathcal{Q}_L$ lies in the region $\mathcal{S}_L^3$. In particular, it lies between $\mathcal{Q}_{A_0C_0}$ and $\mathcal{Q}_H$ in the third quadrant if $1 < \alpha + \beta < \kappa$.*

Proof. We still discuss two cases: (i) $\kappa < \alpha + \beta < 1$ or $\alpha + \beta < \min\{1, \kappa\}$ and (ii) $1 < \alpha + \beta < \kappa$. As known in Theorem 4, for $(\mu_1, \mu_2) \in \mathcal{Q}_{A_0C_0}$ system (3.6) has no equilibria in the interior of the first quadrant, implying that no closed orbits exist in the first quadrant. On the other hand, for $\mu :=$

$(\mu_1, \mu_2) \in \mathcal{S}_L$ system (3.6) has a closed orbit in the first quadrant by Theorem 6. Thus, the continuity of the vector field implies that in case (i) there exists a parameter boundary $\mathcal{Q}_L$ between the curves $\mathcal{Q}_{A_0C_0}$ and $\mathcal{Q}_H$ in $\mathcal{S}_L^3$, as shown in Fig. 2, on which the closed orbit disappears. Obviously, $\mathcal{Q}_L$ cannot coincide with $\mathcal{Q}_H$. In what follows we prove that $\mathcal{Q}_L$ does not coincide with $\mathcal{Q}_{A_0C_0}$ and a heteroclinic loop Γ_L exists when $\mu \in \mathcal{Q}_L$.

For $\mu \in \mathcal{S}_L^3$, both A_0 and A_1 are saddles. Let $\Gamma(\mu)$ denote the limit cycle of system (3.6) for a given $\mu \in \mathcal{S}_L$. By the continuous dependence of solutions on parameters, the limit $\Gamma(\hat{\mu}) = \lim_{\mu \to \hat{\mu} \in \mathcal{Q}_L} \Gamma(\mu)$ is an invariant set. Obviously, $\Gamma(\hat{\mu})$ is also connected. Since Theorem 8 implies that $\Gamma(\mu)$ is stable, i.e., the ω-limit set of an orbit, we can see that $\Gamma(\hat{\mu})$ is also an ω-limit set of an orbit, whose positive semi-orbit is bounded because the two equilibria at infinity in the first quadrant are both repellent. A corollary of the Poincaré–Bendixson Theorem (Theorem 1.3, Chapter II, [11]) implies that $\Gamma(\hat{\mu})$ is either a single equilibrium which has to be C_0, a closed orbit, or a closed curve containing equilibria and a set of orbits connecting these equilibria. However, $\Gamma(\hat{\mu})$ is not C_0 because C_0 remains an α-limit set of an orbit. The definition of $\mathcal{Q}_L$ prevents $\Gamma(\hat{\mu})$ from being a closed orbit. For the third option, the only candidates of equilibria in the closed curve $\Gamma(\hat{\mu})$ are O, A_0 and A_1. By the qualitative properties of these equilibria, the curve $\Gamma(\hat{\mu})$ contains a heteroclinic orbit from A_1 to either O or A_0. Assume it contains the orbit from A_1 to O. Then the saddle A_0 has a stable manifold $W^s_{A_0}$ connecting with C_0. As μ is sufficiently close to the curve $\mathcal{Q}_L$ on the side of existence, the limit cycle $\Gamma(\mu)$ exists and passes through a sufficiently small neighborhood of A_0 close to the curve $\Gamma(\hat{\mu})$, but the stable manifold $W^s_{A_0}(\mu)$ of the saddle A_0 is also close to $W^s_{A_0}$. It turns out to contradict the fact that $W^s_{A_0}(\mu) \cap \Gamma(\mu) \neq \emptyset$. Therefore, $\Gamma(\hat{\mu})$ is a closed curve consisting of saddles A_1 and A_0 and the heteroclinic orbits as shown in Fig. 2, called a heteroclinic loop and denoted by Γ_L. Actually, the boundary $\mathcal{Q}_L$ defines a bifurcation curve for the heteroclinic loop.

Now we can see that the bifurcation curve $\mathcal{Q}_L$ cannot coincide with the bifurcation curve $\mathcal{Q}_{A_0C_0}$. Otherwise, when parameters lie on $\mathcal{Q}_{A_0C_0}$, the equilibrium C_0 coincides with the unstable node A_0. Therefore, the unstable manifold of the saddle A_1 in the first quadrant has to extend to the equilibrium O at the origin, which implies that the heteroclinic loop Γ_L connecting A_0 and A_1 does not exist. This contradicts the existence of heteroclinic loop Γ_L when parameters lie on $\mathcal{Q}_L$.

Case (ii) can be discussed similarly. The proof is completed. □

7. Bifurcation diagrams

Summarizing the above theorems, we can give bifurcation diagrams for parameters μ_1, μ_2 and the corresponding phase portraits for system (3.6) in terms of α, β and κ.

(C1) $\beta < \kappa$, $\alpha < 1$, $\alpha\kappa + \beta - \kappa < 0$ and $1 < \alpha + \beta < \kappa$ (see Fig. 2).
(C2) $\beta < \kappa$, $\alpha < 1$, $\alpha\kappa + \beta - \kappa < 0$ and $\kappa < \alpha + \beta < 1$ (see Fig. 3).
(C3) $\beta < \kappa$, $\alpha < 1$, $\alpha\kappa + \beta - \kappa < 0$ and $\alpha + \beta < \min\{1, \kappa\}$ (see Fig. 4).
(C4) $\beta < \kappa$, $\alpha < 1$ and $\alpha\kappa + \beta - \kappa > 0$ (see Fig. 5).
(C5) $\beta < \kappa$, $\alpha > 1$, $\alpha\kappa + \beta - \kappa > 0$ and $\tilde{a}_{20} < 0$ (see Fig. 6).
(C6) $\beta < \kappa$, $\alpha > 1$, $\alpha\kappa + \beta - \kappa > 0$ and $\tilde{a}_{20} > 0$ (see Fig. 7).
(C7) $\kappa < \beta$, $\alpha < 1$, $\alpha\kappa + \beta - \kappa > 0$ and $\tilde{a}_{20} > 0$ (see Fig. 8).
(C8) $\kappa < \beta$, $\alpha < 1$, $\alpha\kappa + \beta - \kappa > 0$ and $\tilde{a}_{20} < 0$ (see Fig. 9).
(C9) $\kappa < \beta$, $1 < \alpha$, $\alpha\kappa + \beta - \kappa > 0$ (see Fig. 10).

Conditions in cases (C1)–(C4) and (C9) naturally imply $\tilde{a}_{20} < 0$.

In the case that the non-degenerate conditions (H_2) and (H_3) (or equivalently the condition (3.7)) are invalid, the versal unfolding of system (2.13) is of codimension $\geqslant 3$. However, those cases of α, β and κ which satisfy (3.7) may include some deformations of such a higher degenerate vector field. So our discussion as above actually gives results of those versal unfoldings of higher codimensions partially.

It has been demonstrated (see [4,5,13,17,18,22,26]) that predator–prey systems with ratio-dependent functional response exhibit very rich and complex dynamics. These dynamical behaviors

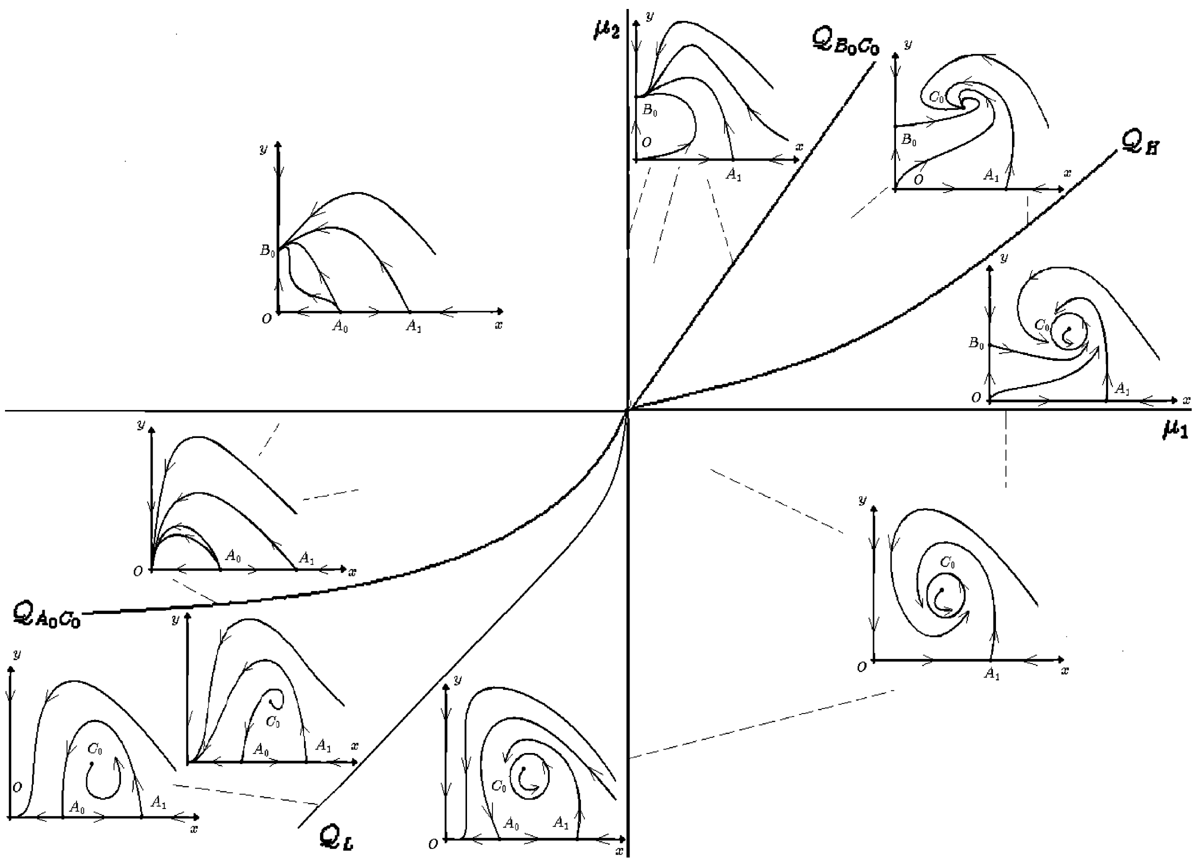

Fig. 3. Bifurcation diagram in case (C2) when $\beta < \kappa$, $\alpha < 1$, $\alpha\kappa + \beta - \kappa < 0$ and $\kappa < \alpha + \beta < 1$.

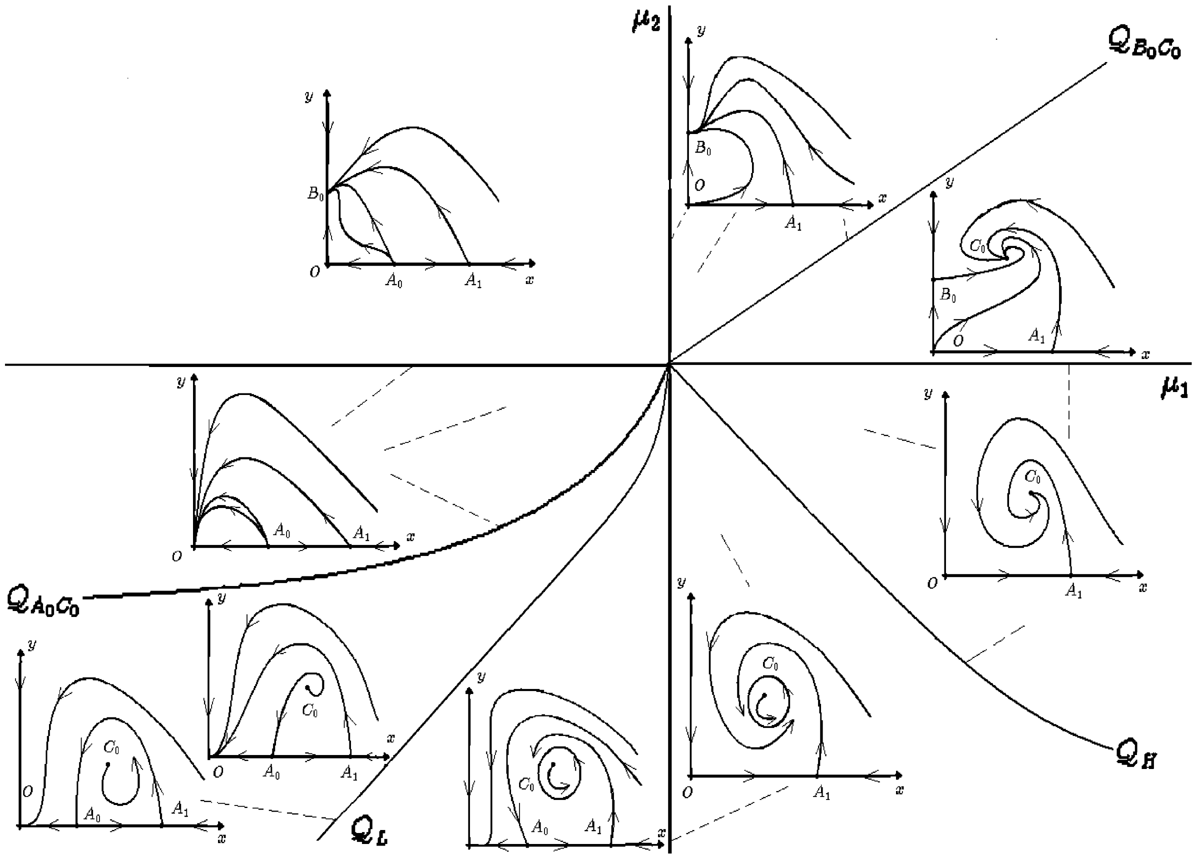

Fig. 4. Bifurcation diagram in case (C3) when $\beta < \kappa$, $\alpha < 1$, $\alpha\kappa + \beta - \kappa < 0$ and $\alpha + \beta < \min\{1, \kappa\}$.

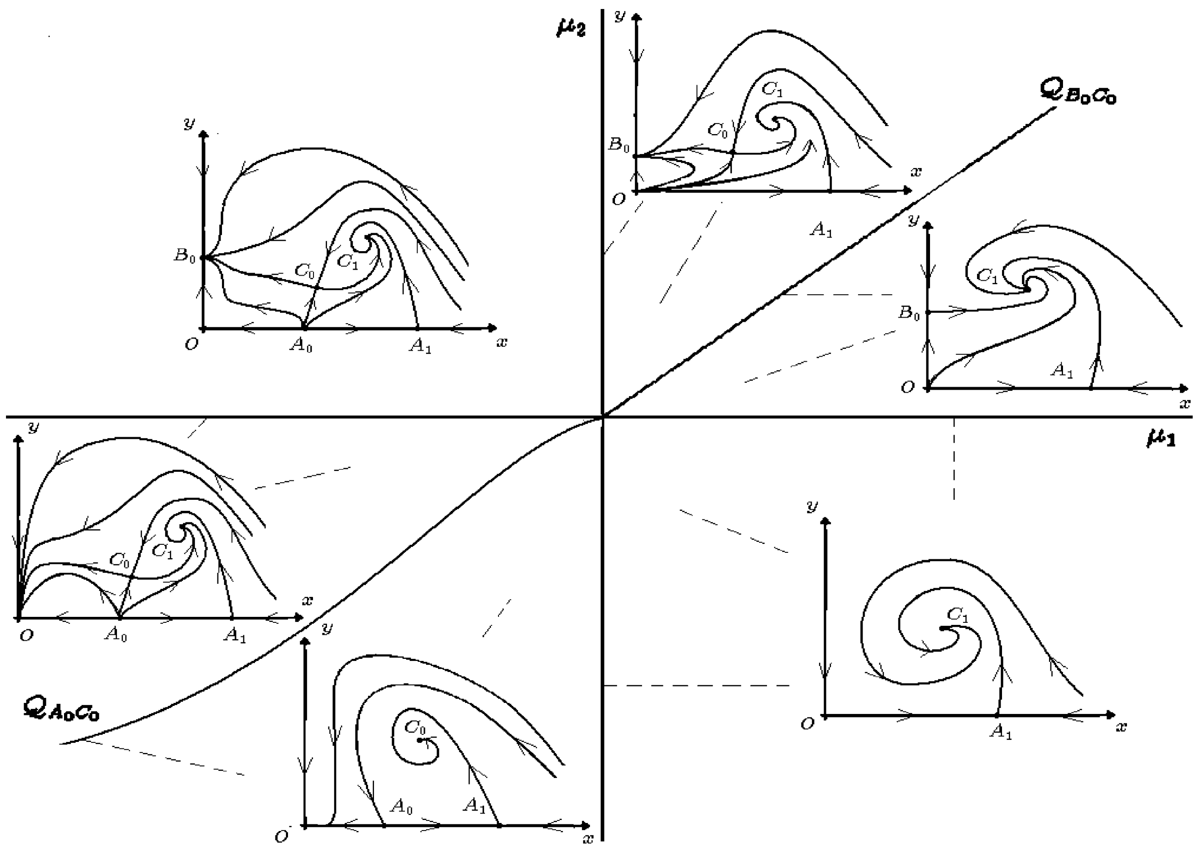

Fig. 5. Bifurcation diagram in case (C4) when $\beta < \kappa$, $\alpha < 1$ and $\alpha\kappa + \beta - \kappa > 0$.

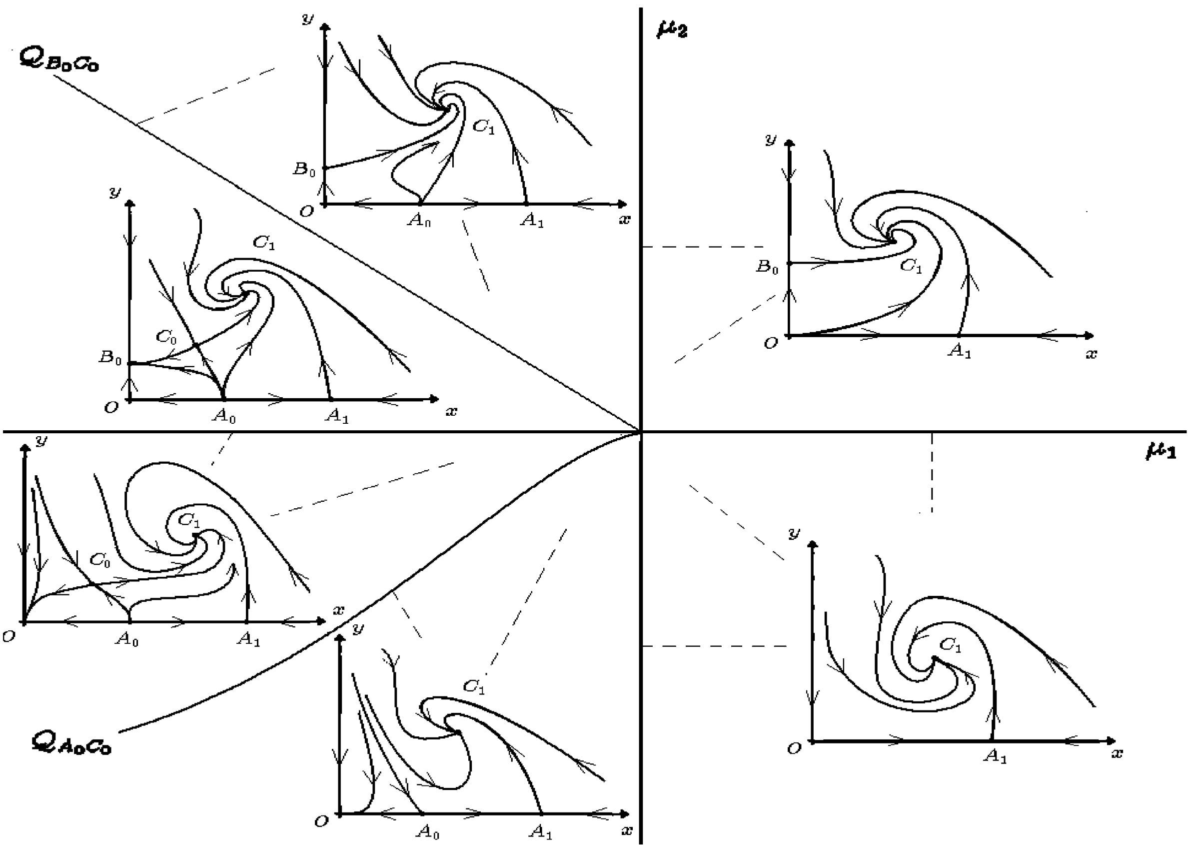

Fig. 6. Bifurcation diagram in case (C5) when $\beta < \kappa$, $\alpha > 1$, $\alpha\kappa + \beta - \kappa > 0$ and $\tilde{a}_{20} < 0$.

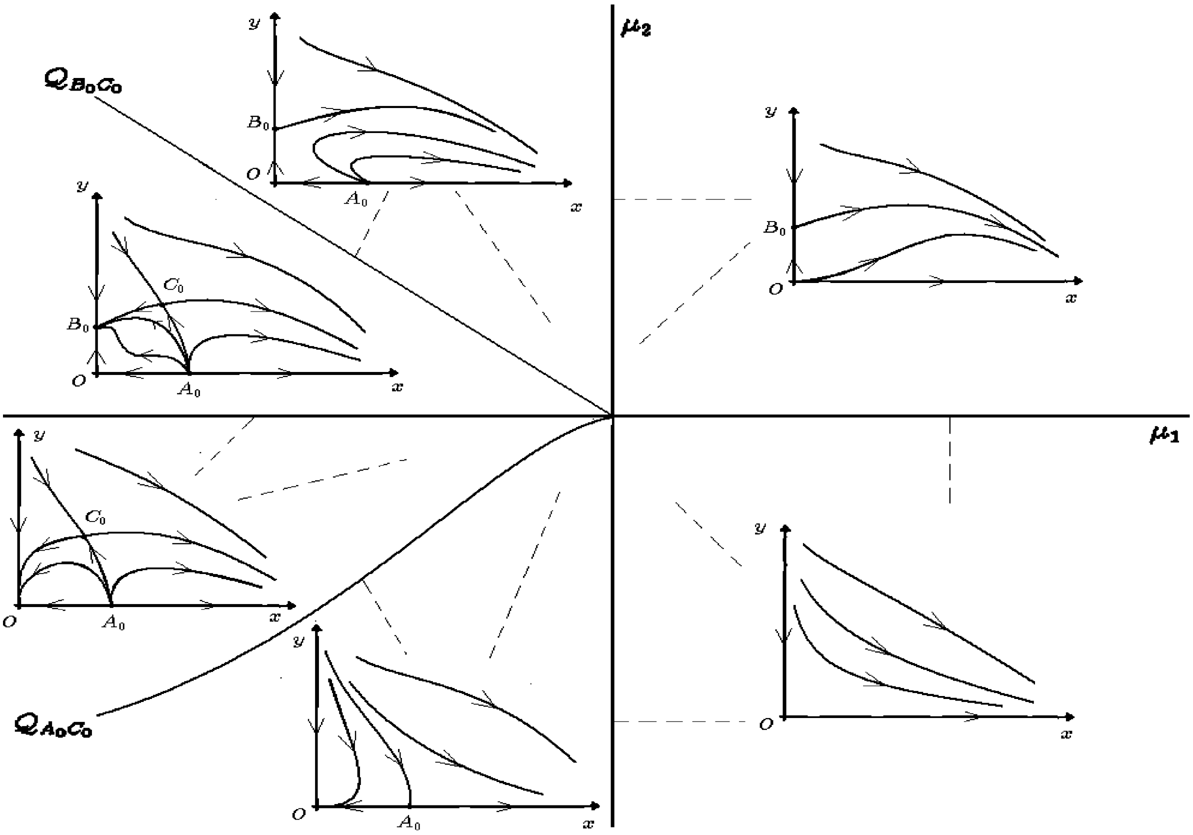

Fig. 7. Bifurcation diagram in case (C6) when $\beta < \kappa$, $\alpha > 1$, $\alpha\kappa + \beta - \kappa > 0$ and $\tilde{a}_{20} > 0$.

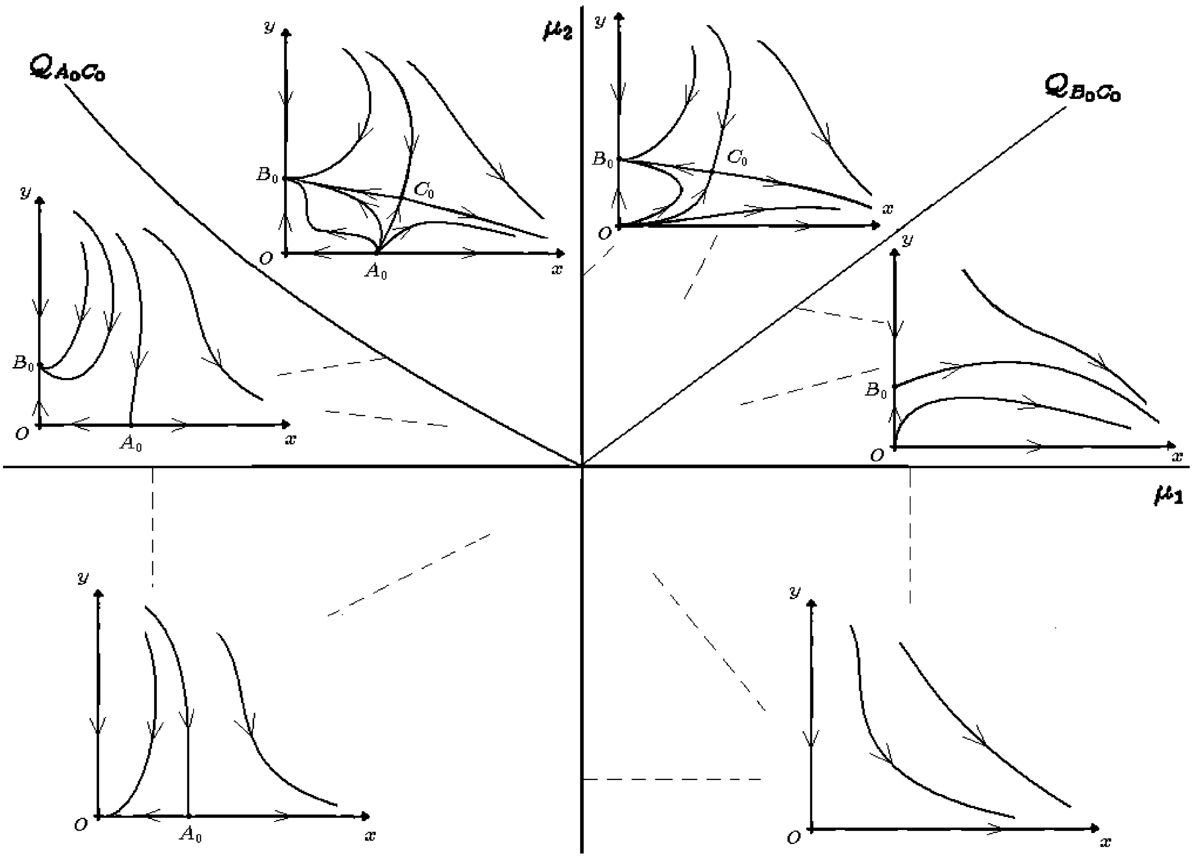

Fig. 8. Bifurcation diagram in case (C7) when $\kappa < \beta$, $\alpha < 1$, $\alpha\kappa + \beta - \kappa > 0$ and $\tilde{a}_{20} > 0$.

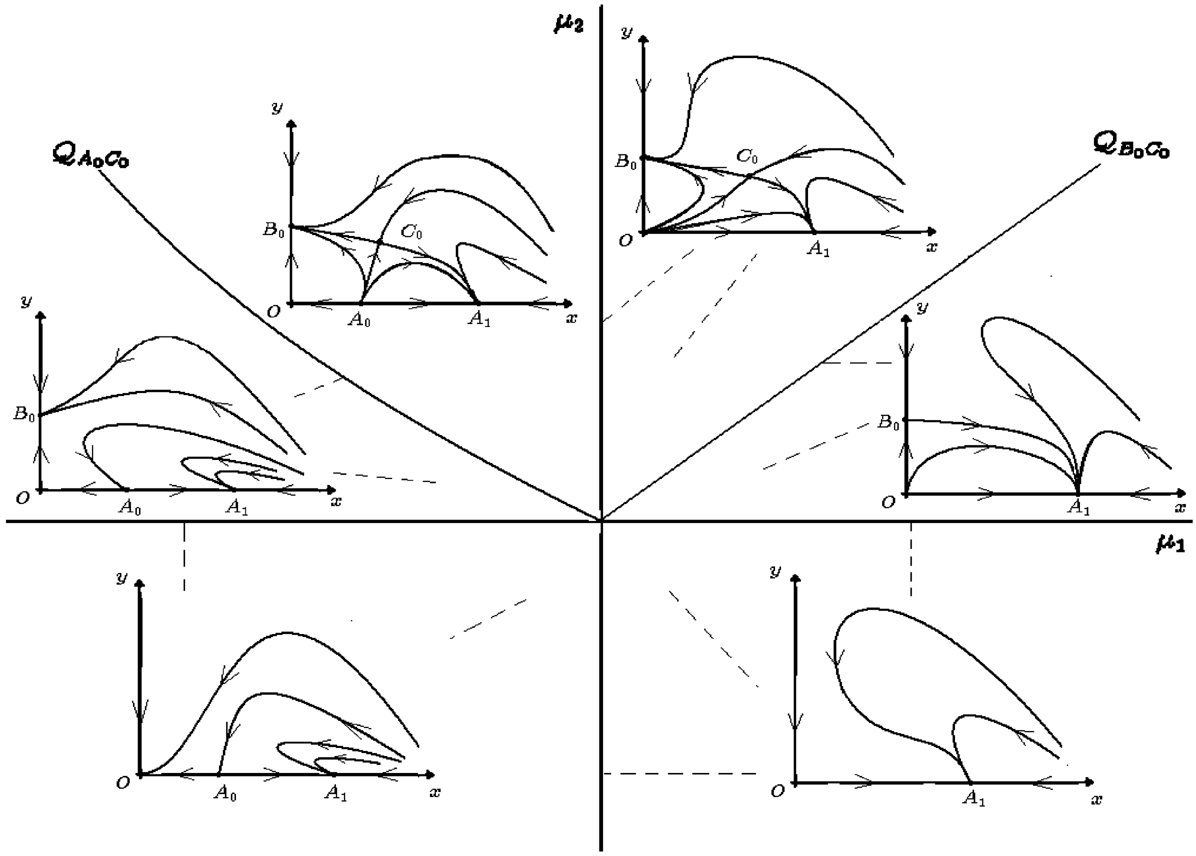

Fig. 9. Bifurcation diagram in case (C8) when $\kappa < \beta$, $\alpha < 1$, $\alpha\kappa + \beta - \kappa > 0$ and $\tilde{a}_{20} < 0$.

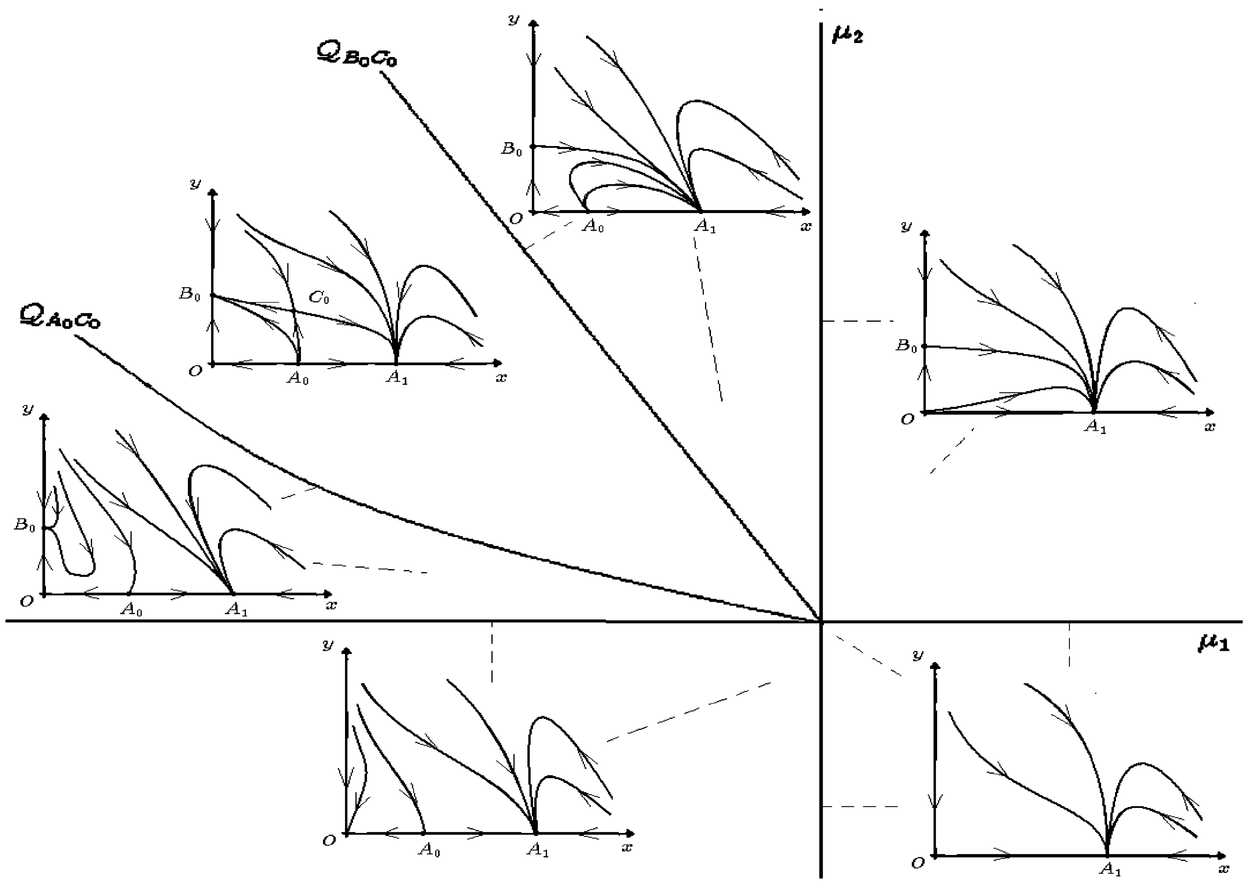

Fig. 10. Bifurcation diagram in case (C9) when $\kappa < \beta$, $1 < \alpha$, $\alpha\kappa + \beta - \kappa > 0$.

are very sensitive to the initial values and the system parameters. These small changes can be understood as small perturbations of the system but are difficult to estimate. An effective approach is to discuss all possible small perturbations and explore its all possible phase portraits. That is the reason we investigate its versal unfoldings.

In the case (C3), for example, the bifurcation diagram is shown in Fig. 3. If (μ_1, μ_2) lies above the bifurcation curve $\mathcal{Q}_{A_0C_0}$ but below the μ_1-axis, all orbits starting from an initial point in the interior of the first quadrant eventually go to the origin. Hence, both the predators and the prey go to extinction. If (μ_1, μ_2) lies below $\mathcal{Q}_{B_0C_0}$ and to the right of the μ_2-axis, the predators and the prey coexist in a regime of fixed populations or periodic oscillations because all orbits in the interior approach an equilibrium C_0 or a stable limit cycle. If (μ_1, μ_2) lies between $\mathcal{Q}_L$ and the μ_2-axis, the orbits above the stable manifold of the saddle A_0 go to the origin but those below approach a stable limit cycle or the heteroclinic loop Γ_L formed with the stable manifold. Therefore, the predators and the prey either both go to extinction or coexist in a regime of bounded oscillations. If (μ_1, μ_2) lies between $\mathcal{Q}_{A_0C_0}$ and $\mathcal{Q}_L$, all orbits go to the origin except the one at the source C_0 or on the stable manifold of the saddle A_0. That is, the predators and the prey generically go to extinction. Similarly, we can explain the other cases (C1)–(C9).

Acknowledgments

The authors are grateful to the anonymous referees for their careful reading and helpful comments.

References

[1] R. Arditi, A.A. Berryman, The biological control paradox, Trends Ecol. Evol. 6 (1991) 32.
[2] R. Arditi, L.R. Ginzburg, Coupling in predator–prey dynamics: ratio-dependence, J. Theoret. Biol. 139 (1989) 311–326.
[3] V.I. Arnold, Geometrical Methods in the Theory of Ordinary Differential Equations, Springer-Verlag, New York, 1983.
[4] F. Berezovskaya, G. Karev, R. Arditi, Parametric analysis of the ratio-dependent predator–prey model, J. Math. Biol. 43 (2001) 221–246.
[5] A.A. Berryman, The origins and evolution of predator–prey theory, Ecology 73 (1992) 1530–1535.
[6] S.-N. Chow, C. Li, D. Wang, Normal Forms and Bifurcation of Planar Vector Fields, Cambridge University Press, Cambridge, 1994.
[7] W.A. Coppel, Quadratic systems with a degenerate critical point, Bull. Austral. Math. Soc. 38 (1988) 1–10.
[8] W.A. Coppel, A new class of quadratic systems, J. Differential Equations 92 (1991) 360–372.
[9] H.I. Freedman, Deterministic Mathematical Models in Population Ecology, Monogr. Textbooks Pure Appl. Math., vol. 57, Marcel Dekker, New York, 1980.
[10] J. Guckenheimer, P. Holmes, Nonlinear Oscillations, Dynamical Systems and Bifurcations of Vector Fields, Springer-Verlag, New York, 1983.
[11] J.K. Hale, Ordinary Differential Equations, second edition, Willey–Interscience, New York, 1980.
[12] M.W. Hirsch, Differential Topology, Springer-Verlag, New York, 1976.
[13] S.-B. Hsu, T.-W. Hwang, Y. Kuang, Global analysis of the Michaelis–Menten-type ratio-dependent predator–prey system, J. Math. Biol. 42 (2001) 489–506.
[14] C.B. Huffaker, Experimental studies on predation: dispersion factors and predator–prey oscillations, Hilgardia 27 (1958) 343–383.
[15] C. Jost, O. Arino, R. Arditi, About deterministic extinction in ratio-dependent predator–prey models, Bull. Math. Biol. 61 (1999) 19–32.
[16] R.E. Kooij, A. Zegeling, A predator–prey model with Ivlev's functional response, J. Math. Anal. Appl. 198 (1996) 473–489.
[17] Y. Kuang, E. Beretta, Global qualitative analysis of a ratio-dependent predator–prey system, J. Math. Biol. 36 (1998) 389–406.
[18] B. Li, Y. Kuang, Heteroclinic bifurcation in the Michaelis–Menten type ratio-dependent predator–prey system, SIAM J. Appl. Math. 67 (2007) 1453–1464.
[19] R.F. Luck, Evaluation of natural enemies for biological control: a behavioral approach, Trends Ecol. Evol. 5 (1990) 196–199.
[20] L.S. Luckinbill, Coexistence in laboratory populations of *Paramecium aurelia* and its predator *Dininium nasutum*, Ecology 53 (1973) 1320–1327.
[21] R.M. May, Stability and Complexity in Model Ecosystem, Princeton Univ. Press, Princeton, 1974.
[22] S. Ruan, Y. Tang, W. Zhang, Computing the heteroclinic bifurcation curves in predator–prey systems with ratio-dependent functional response, J. Math. Biol. 57 (2008) 223–241.
[23] G. Sansone, R. Conti, Non-Linear Differential Equations, Pergamon Press, New York, 1964.
[24] Y. Tang, W. Zhang, Generalized normal sectors and orbits in exceptional directions, Nonlinearity 17 (2004) 1407–1426.
[25] Y. Tang, W. Zhang, Heteroclinic bifurcation in a ratio-dependent predator–prey system, J. Math. Biol. 50 (2005) 699–712.
[26] D. Xiao, S. Ruan, Global dynamics of a ratio-dependent predator–prey system, J. Math. Biol. 43 (2001) 268–290.
[27] Z.-F. Zhang, Proof of the uniqueness theorem of limit cycles of generalized Liénard equations, Appl. Anal. 23 (1986) 63–76.
[28] Z.-F. Zhang, T.-R. Ding, W.-Z. Huang, Z.-X. Dong, Qualitative Theory of Differential Equations, Transl. Math. Monogr., vol. 101, Amer. Math. Soc., Providence, 1992.